Oxidative degradation of amine solvents for CO_2 capture

By:

Hanbi Liu
Daniel Hatchell
Omkar A. Namjoshi
Gary T. Rochelle

ACKNOWLEDGEMENTS

I would like to thank my research advisor, Gary Rochelle, for his mentorship and guidance. The two years spent in his lab is truly the greatest highlight of my undergraduate career.

I would also like to thank my graduate student, the greatest teacher, mentor, counselor and friend, Omkar Namjoshi. You are one of the most intelligent and knowledgeable people I have encountered. I would not have achieved my professional and academic success today without your tireless investment.

It has also been a pleasure to work my research partner, Daniel Hatchell. I am truly impressed by your intelligence and success as a researcher, and I am sure your talents will shine in your future careers.

The graduate students in Dr. Rochelle's lab – Kent Fischer, Paul Nielsen and Nathan Fine – have been valuable sources of technical advice. I appreciate your guidance and contributions to this project, and I have enjoyed my daily interactions with each and every one of you.

Last, but not the least, I would like to thank my family and friends for their support and being such great listeners when I needed their inputs. My thanks go especially to Heather Bolton and Han Tu for their help in running the experiment in the last semester of my research.

All of you have been integral parts of my undergraduate career at UT Austin, and I am humbled to have known you. I hope I have reciprocated your invaluable gifts with whatever little contributions I can offer, and I hope you will be successful in your future pursuits.

ABSTRACT

This thesis focuses on the oxidative degradation of amine solvents used in coal-fired power plant flue gas CO_2 capture. The relationship between amine structures and their oxidative degradation was studied at low temperature absorber conditions in order to identify stable amines that should be more rigorously screened. Amongst primary amines, those with three carbons separating the amino group from the neighboring electron-withdrawing group (such as PDA and MPA) showed resistance to oxidation, while those with even number of carbons (such as MEA, EDA, and DGA®) were susceptible to oxidation. Secondary amines did not follow the same observations. Tertiary amines resisted oxidation regardless of the structural characteristics mentioned above. The production of major oxidation products such as formate, oxalate and nitrite closely track parent amine degradation. Formate and oxalate are produced in certain ratios, and the ratio is different depending on the amine. Amine loss and formate also approach a certain ratio over time. The mechanism of oxidation is currently not well understood, and these observations are important to understanding the mechanisms of oxidation, production of nitrosamines from oxidation, and explaining why certain structures are resistant or susceptible to oxidation.

Table of Contents

List of Figures

List of Tables

INTRODUCTION

Motivation for CO_2 Capture

As concerns over climate change grow among industrialized nations, so does the need to regulate CO_2 emission. CO_2 is one of the main contributors to global warming. The Clean Air Act of 2007 allowed the US executive branch to regulate CO_2 emissions. Other industrialized countries have launched carbon tax and cap-and-trade programs that place a hard limit on total annual emission (Namjoshi, 2015). In 2013, CO_2 accounted for 82% of all US greenhouse gas emissions. Combustion of fossil fuel for energy and transportation are the main sources of CO_2 emission. Electricity is a significant source of energy and accounts for 37% of total US CO_2 emissions (EIA, 2014). Carbon capture and storage technology offers a way to reduce emission from point sources such as power plant flue gas by capturing, compressing and sequestering the CO_2 into depleted reservoirs and geological formations.

Amine Scrubbing Overview

Amine scrubbing is a technology first proposed in the 1930's that separates sour gases such as H_2S, COS, and CO_2 from process streams using aqueous amine solutions. This technology has already been applied to various industrial applications such as refining and natural gas processing. Compared to other technologies for flue gas CO_2 capture such as oxycombustion and membrane separation, amine scrubbing is more mature, more efficient, better-understood and easier to retrofit onto existing plants. Figure 1 shows a flow sheet of the process.

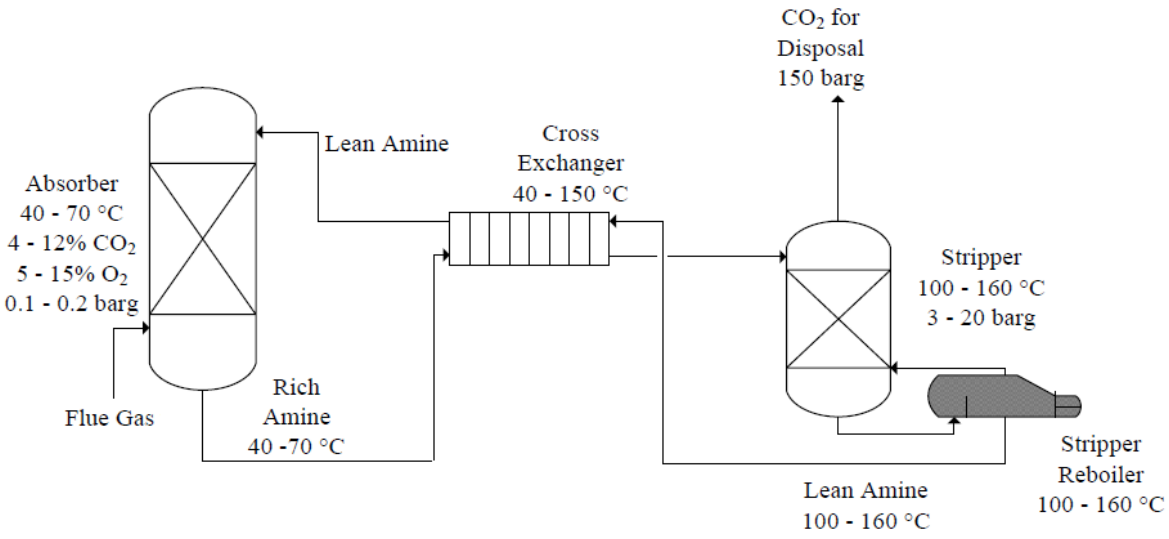

Figure 1. Process flow diagram of CO_2 Capture from flue gas with stream conditions (Namjoshi, 2015)

Flue gas enters the absorber column at the bottom. The concentration for CO_2 can range from 4 – 12% for CO_2 and 5 – 15% for O_2 depending on fuel source. The lower CO_2 concentration corresponds to natural gas and higher concentration corresponds to coal. Aqueous amine solvents chemically absorb the CO_2 and leave the absorber as rich amine at 40 – 70 ℃. Scrubbed gas leaves the absorber column from the top where a water wash removes volatile components and scrubbed gas is discharged into the atmosphere. The rich amine is pre-heated in a cross-exchanger and enters the stripper where CO_2 is stripped out at high temperature and sent to compression and storage. The amine solution, now with CO_2 removed, is recycled back through the cross-exchanger and enters the absorber where the cycle repeats.

Several issues exist in solvent management for long-term cycling operations. Thermal degradation of the solvent due to high temperature in the stripper and oxidative degradation due to reaction with oxygen in the absorber column are two of the greatest contributors to solvent loss. 70% of the total amine loss can be attributed to oxidation, 30% to thermal degradation, with minimal percentages from volatility and reclaiming losses. If the power plant uses natural gas as fuel, higher O_2 partial pressure in the flue gas makes oxidation an even greater issue. Degraded solvents have reduced CO_2 absorption rate and CO_2 cyclic capacity. Oxidative degradation produces volatile amine, small amounts of nitrosamine, and thermal degradation produces high-molecular weight polyamines and substitution products. Most of the nitrosamine is produced from NOx in the flue gas. Nitrosamine is a known carcinogen and volatile amines can produce aerosols which poses a hazard to human health and the environment. The environmental impacts of high-molecular thermal degradation products are not yet well understood. In addition to environmental concerns, reclaiming degraded solvents and solvent make up may account for 10% of the operating cost (Rao and Rubin, 2002). Operating costs and environmental impacts of degradation products are the main motivations that drive the need to better understand and minimize degradation.

Literature Review

Several researchers including Goff (Goff, 2005), Sexton (Sexton, 2008) and Voice (Voice, 2013) have worked with oxidative degradation in the past. Goff focused on the mass transfer aspect of oxidation and pointed out that previous experiments on oxidation were mass-transfer limited. Sexton focused on characterizing MEA (ethanolamine) degradation products. He identified two major oxidative degradation products, 1-(2-hydroxyethyl)-formamide (HEF) and 1-(2-hydroxyethyl)-imidazole (HEI). Voice closed material balance for low and high temperature MEA oxidation. He also expanded studies on the effects of metal catalysts, chelating agents, and inhibitors. Voice included amine screening in the high gas flow apparatus. The High Gas Flow apparatus (HGF) uses a FTIR (Fourier Transform Infrared Spectroscopy) to instantaneously determine concentration of ammonia in the liquid sample, assuming all ammonia is produced from oxidation. The HGF uses a much higher gas rate (7.65 SLPM) and yields lower degradation rate due to lack of agitation and the use of air rather than oxygen. Nevertheless, the trends observed in HGF should be similar to that observed in the Low

Gas Flow apparatus used in this study (LGF). The main advantage to LGF is that it allows for regular liquid sampling, including endpoints at the beginning and end of experiment.

The mechanistic pathway of oxidation is not well-understood. Some proposals exist for MEA oxidation, which mainly proceeds by radical chain mechanisms. Organic hydroperoxides called MEA-hydroperoxide (MEA-HP) forms at absorber conditions by reacting with oxygen. MEA-HP can generate free-radicals and each new free radical will react with MEA and oxygen to produce another MEA-HP molecule or propagate the chain reaction by generating another free radical. Oxidation pathways of other amines are still unknown, but major oxidation products such as heat stable salts and ammonia have been used as means to study oxidative degradation (Voice, 2013).

Oxidation can be kinetically controlled or mass-transfer controlled. Oxygen concentration at steady state is different in gas and liquid phases. Figure 2 from Goff illustrates this idea in terms of oxygen concentration and partial pressure.

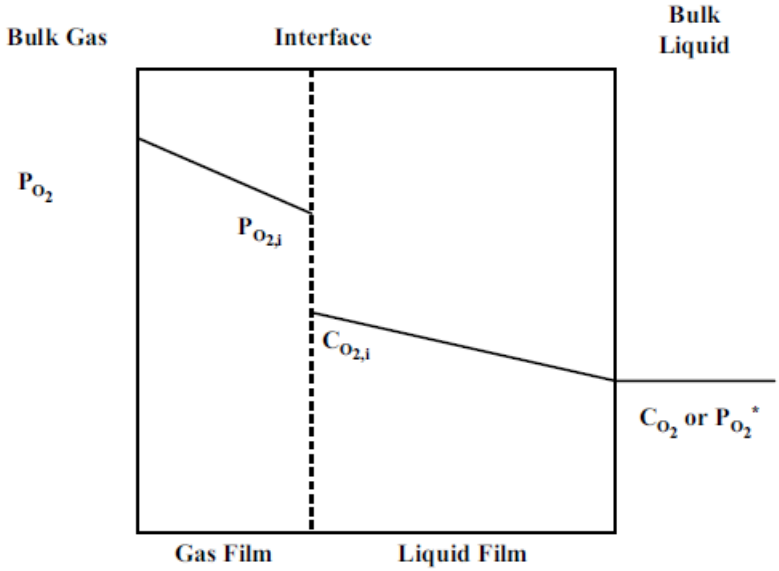

Figure 2. Concentration Profile for Physical Absorption of O_2 into MEA (Goff, 2005)

There are five different regimes of mass transfer with chemical reaction: Kinetic, Diffusion, Fast Reaction, Instantaneous Reaction, and Surface Reaction. The kinetic regime controls rate of degradation when bulk liquid is saturated with oxygen, and kinetics only depends on reactant or catalyst concentration. As rate of reaction increases, the reaction takes places away from the bulk liquid and eventually moves to the gas film where reaction takes place instantaneously. Degradation rate is controlled by diffusion of oxygen to the phase where reaction takes place. In this study, most of the trials were kinetically controlled. Diffusion regime only takes place when an amine oxidizes severely and this is not frequently observed in low temperature experiments.

Sexton (2008) performed many MEA oxidation experiments in the LGF reactor with different amine, catalyst and inhibitor combinations. He tested DEA

(diethanolamine) and DGA® (diglycolamine®) and found that unloaded 4 m DEA and DGA solutions are resistant to oxidation. Screening works by Voice using the high gas flow apparatus at 55 or 70 ℃ has seen Jeffamine® (bis(2-aminoethyl)ether), MAPA (3-(methylamino)propylamine), MAE (methylaminoethanol), DGA and EDA (ethylenediamine) degraded at a rate equal or higher than that of MEA. These amines all produced volatile products (NH_3) in the presence of inhibitor A. Voice showed that HMDA (hexamethylenediamine) was less susceptible to oxidation than MEA. MPA (3-amino-1-propanol), PE (2-piperidineethanol) and DAB only degraded and produced volatile products in the presence of Cu, a potent catalyst. All tertiary amines were found to resist oxidation at low temperatures. Voice concluded that number of carbons between nucleophilic groups is important in determining oxidative stability. His work also found that the same metals can act as a catalyst or an inhibitor depending on the amine. For example, Fe suppressed oxidation in EDA and MAPA and inhibitor A enhanced oxidation in DGA. Inhibitor A was not included in this study, but 0.4 mM of Fe^{3+}, 0.2 mM Mn^{2+}, 0.1 mM Ni^{2+}, and 0.05 mM Cr^{3+} were included as catalysts for degradation.

Voice also screened amines using the Integrated Solvent Degradation Apparatus (ISDA). The ISDA simulates oxidative and thermal degradation with high temperature cycling, similar to real systems. Voice showed that amines that did not undergo oxidation at absorber conditions without high temperature cycling such as such as AMP (2-amino-2-methyl-1-propanol), PZ and PZ-promoted MDEA (Methyl diethanolamine) showed various degrees of degradation in the ISDA. Oxidation continued after dissolved oxygen is depleted, suggesting that high temperatures will increase oxidation regardless of whether there is dissolved oxygen in the bulk solution. Fast reacting intermediates may be present at high stripper temperatures. These intermediates enhance oxygen mass transfer in the absorber, accelerating oxidation. Therefore, high temperature cycling is necessary to understand high temperature oxidation of amines that are stable at low temperatures.

Scope

This thesis focuses on the oxidative degradation of amine solvents used in coal-fired power plant flue gas CO_2 capture. Degradation of amines was conducted in the Low Gas Flow reactor that simulates absorber conditions. Rate constants of oxidation were reported but the numerical values were not rigorously obtained. The repeatability of the experiments was not tested, and the regression fits do not always yield satisfactory R^2 values. Voice previously tested many amines included in this study, but Voice did not conduct screening at consistent conditions and thus results could not be used for direct comparisons. This work tested all amines at consistent conditions and results are more reliable for comparisons on these amines' susceptibility to oxidative degradation. Rates of amine degradation and rate of formate, oxalate and nitrite formation are presented, and conclusions are drawn on the relationship between amine structures and their oxidative degradation behaviors in order to identify stable amines that should be more rigorously screened.

METHODOLOGY AND SCOPE

Solution Preparation

Solutions were prepared gravimetrically. The solvents were made by first mixing amine with water in a glass bottle using a digital scale with an accuracy of 0.1 g. Table 1 shows all amines screened in this study. Most amines used in this study are liquids at room temperature and can be transferred into the glass bottle using a funnel. The only exceptions are piperazine which is a flaky solid at room temperature and HMDA which is amorphous at room temperature and needed to be heated in a water bath prior to solution preparation. Monoamine solutions were prepared at 10 m, diamine solutions at 5 m and tertiary amine blends at 3.33 m with 3.33 m PZ as rate promoter. The goal is to keep solution alkalinity at a constant 10 m across all trials.

CO_2 was loaded by sparging CO_2 into the solution using a gas washing bottle. Target CO_2 loading was 0.4 mol CO_2/mol alkalinity for all monoamine and diamine solutions. The target loading for DMAE and DMAP blend with PZ was 0.25 mol CO_2/mol alkalinity. For detailed procedure on solvent preparation, refer to Namjoshi section 3.2 (Namjoshi, 2015). Table 1 shows all amines tested in this study and

Table 1. Amines Tested

Amine	Abbreviation	MW	Structure
Propylenediamine	PDA	74.12	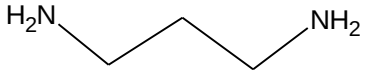
Ethylenediamine	EDA	60.10	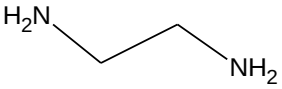
1,4-diaminobutane	DAB	88.15	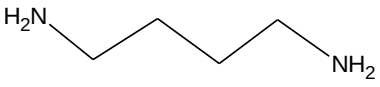
Hexamethylenediamine	HMDA	116.21	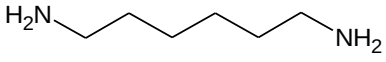
3-Amino-1-propanol	MPA	75.11	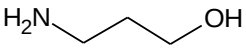
Diglycolamine®	DGA®	105	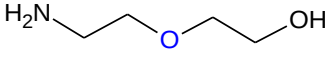

Bis(2-aminoethyl) Ether	Jeffamine®	104.15	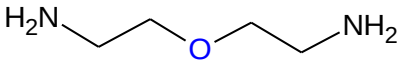
Diethanolamine	DEA	105.14	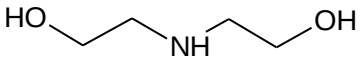
Methylaminoethanol	MAE	75.11	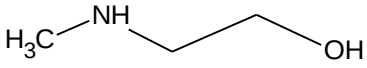
Ethanolamine	MEA	61.08	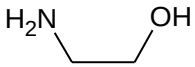
3-(Methylamino)propylamine	MAPA	88.15	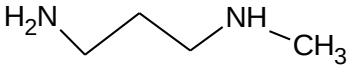
2-Dimethylaminoethanol	DMAE	89.14	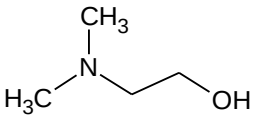
3-Dimethylamino-1-propanol	DMAP	103.16	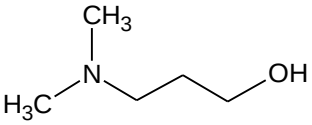

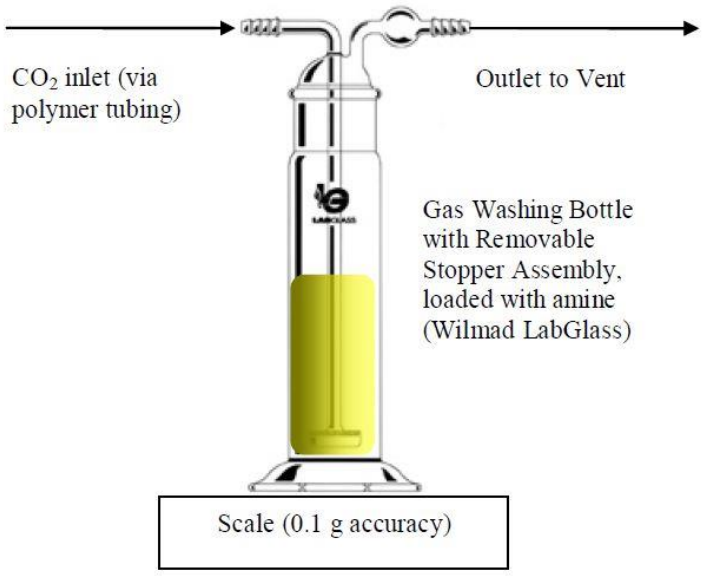

Figure 3. CO2 loading apparatus used to add CO2 to amine solution (Namjoshi, 2015)

Oxidative Degradation Apparatus

The solutions were degraded in the low gas flow (LGF) reactor which simulates absorber conditions. The reactor was a semi-batch jacketed glass reactor that is mechanically agitated by a motor with impeller. It is first developed by Sexton (2008) to accelerate oxidation at high oxygen concentration to observe degradation and product formation over one to two weeks (Voice, 2013). A schematic of the low gas flow apparatus is shown below.

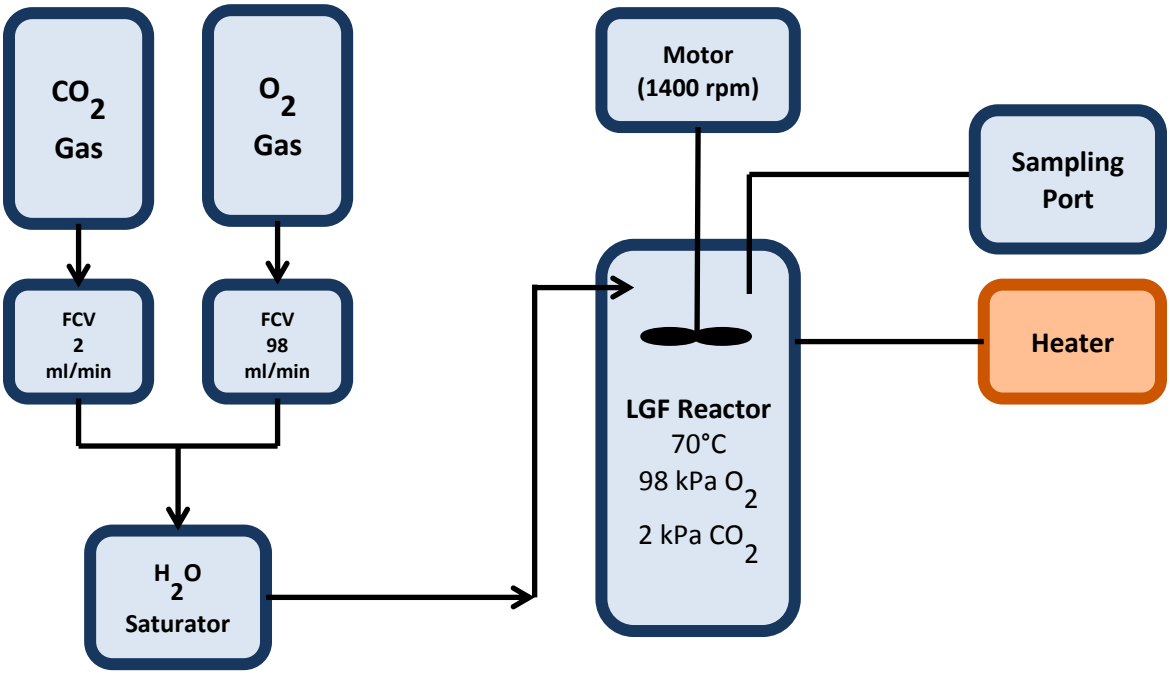

Figure 4. Low gas flow oxidation apparatus used in the experiment

The reactor is filled with 350ml of amine solution. 0.4 mM of Fe^{3+}, 0.2 mM Mn^{2+}, 0.1 mM Ni^{2+}, and 0.05 mM Cr^{3+} are added to the solution. The reactor head was sealed with a Teflon® cap. The reactor was agitated at 1400 rpm by a motor with stainless steel impeller and heated at 70 ^{o}C by circulating mineral oil in the jacket. Carbon dioxide and oxygen from their respective gas cylinders were passed through two calibrated mass flow controls to maintain a reactor pressure of 98 kPa O_2 and 2 kPa CO_2. The O_2/CO_2 mixture was saturated with water before being fed to the reactor through the Teflon® cap to make up water loss due to evaporation. The reactor has level marks that indicated solution level, and roughly 4 ml of water per 1 - 2 days needed to be added to maintain constant liquid level.

Samples are taken out of the reactor through the sampling port with a pipet based on the following schedule.

Table 2. General sampling schedule of oxidation experiments

Sample number	Time since start of experiment
1	At starting time
2	1 day
3	2 day
4	3 days
5	4~5 days
6	6~7 days
7	9~10 days
8	13~14 days

Analytical methods

Cation chromatography and anion chromatography were used to determine the concentration of amine and degradation products. Results from both chromatographs are analyzed with Chromeleon^{TM} 6.8 software.

For every amine or degradation product analyzed in cation and anion chromatography, a standard curve of peak area vs. concentration is needed. Samples with known amine/product concentration are made and analyzed with the chromatographs, and a quadratic fit calibration curve is generated. This curve will be used to convert peak areas into concentrations of amine/product in the degraded samples.

Cation Chromatography

Cation chromatography was used to analyze the concentration of amines in degraded samples. The degraded amine samples are diluted by a factor of 10,000 with DDI before analysis. A Dionex ICS-2100 chromatography with CS17 analytical column (4 x 250 mm) was used. The eluent is DDI and a gradient of methylsulfonic acid (MSA) from 0 – 100 mM. The methods employed in this study are similar to those of Namjoshi (2015). For more detailed explanation on the mechanisms of cation chromatography and the calculations leading to final results, refer to Namjoshi (2015).

Anion Chromatography

Amine oxidation produces organic acids and anionic species. In this study, Dionex ICS-3000 anion with AS15 analytical column (4 x 250 mm) and potassium hydroxide eluent was used to resolve the amount of anionic products in diluted samples. The species analyzed in this study are formate, oxalate and nitrite. Degraded amine samples are first hydrolyzed with roughly 0.03 g of 98% NaOH, or twice the mass of amine. This process converts all neutral-charged degradation products to undegraded amines and anions that can be detected by the instrument. After one day, the hydrolyzed amine samples are diluted by a factor of 100 with DDI (0.015 g amine, 0.03 g NaOH and 1.5 g DDI). The following figure shows an example of the hydrolysis reaction.

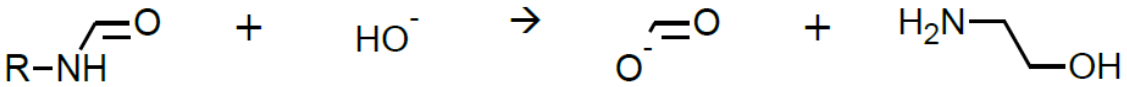

Figure 5. Hydrolysis of formyl amides by treatment with NaOH (Voice, 2013)

The standards for anion chromatography are also hydrolyzed with 0.03 g NaOH, same as the amount in hydrolyzed amine samples. The NaOH in degraded samples delay elution time and the same has to be done for the standards to better match the elusion times. This improves peak area calculation and leads to a better calibration curve. The following figure shows the chromatograph peaks for 188 ppm formate, 69 ppm nitrite and 343 ppm oxalate standard. A calibration curve is constructed from standard sample peak areas in the anion chromatography and standard concentrations from dilution. The calibration curve can be used to calculate heat stable salts concentrations in degraded samples given peak areas in these samples. The calculations leading to final results are similar to those for cation chromatography.

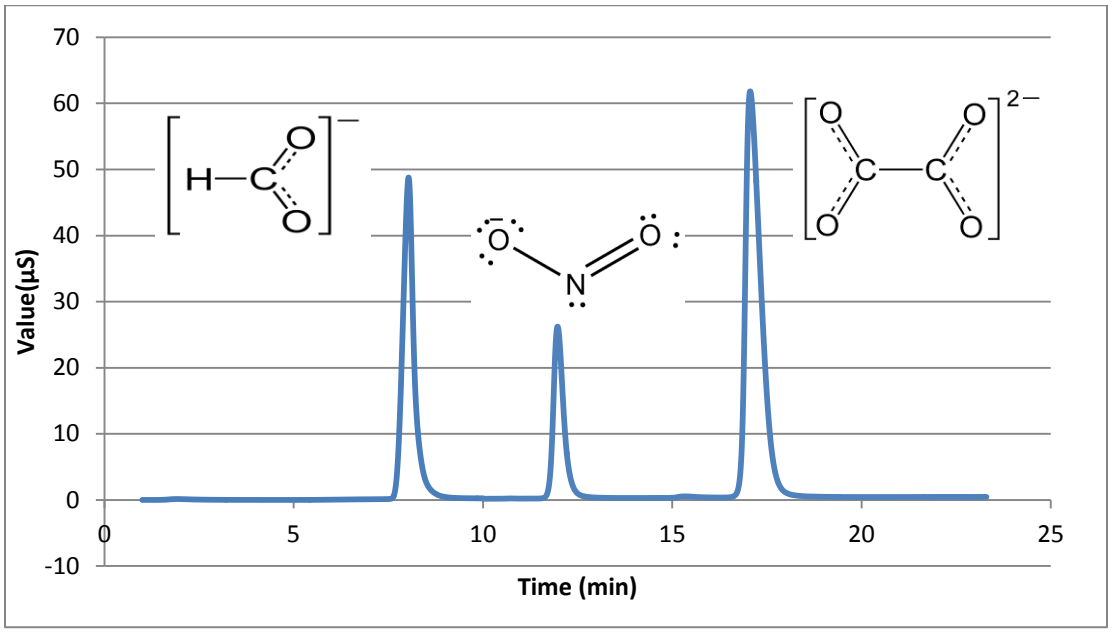

Figure 6. Formate, nitrite and oxalate standard

RESULTS

10 m Ethanolamine (MEA)

MEA was tested as a benchmark for comparison because MEA oxidation is most-studied among all other amines. MEA shows significant initial degradation that follows 1st order kinetics and then reaches equilibrium after roughly 120 hours. The rate constant is 0.015 hr^{-1} and about 78% of the amine was lost by the end of the experiment. Only the first four data points are used to fit first-order rate law.

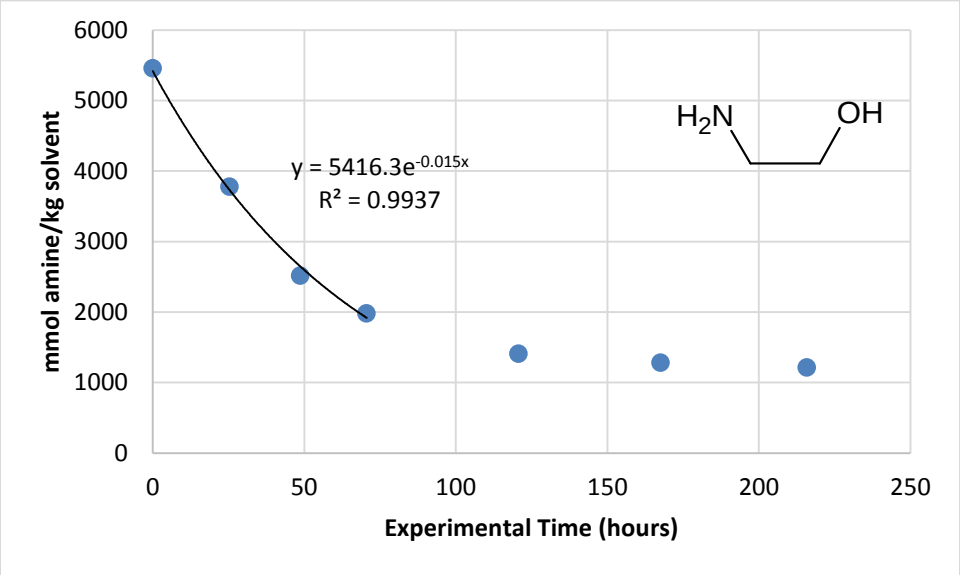

Figure 7. Oxidation of 10 m MEA. 70 ℃, 98 kPa O2, 2 kPa CO2, 100 ml/min gas flow, 1400 rpm , 0.4 mM of Fe^{3+}, 0.2 mM Mn^{2+}, 0.1 mM Ni^{2+}, and 0.05 mM Cr^{3+}.

Oxalate formation in MEA degradation reached a peak then decreased, indicating that oxalate may be an intermediate product in MEA oxidation.

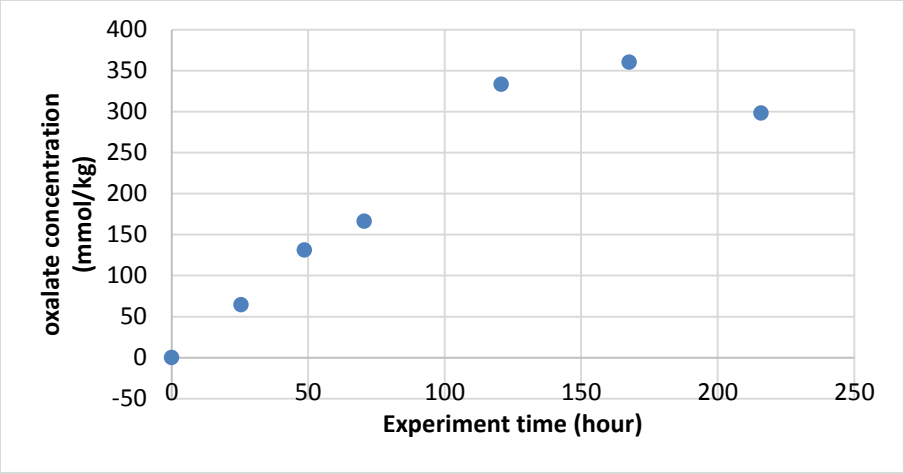

Figure 8. Oxidation product (oxalate) of 10 m MEA. 70 ℃, 98 kPa O2, 2 kPa CO2, 100 ml/min gas flow, 1400 rpm , 0.4 mM of Fe^{3+}, 0.2 mM Mn^{2+}, 0.1 mM Ni^{2+}, and 0.05 mM Cr^{3+}.

Formate concentration increased steadily over time, reached equilibrium, and continued to increase until end of experiment. Trend of formate production corresponds to the trend of MEA degradation. Unlike oxalate concentration, which decreased in the last sample, formate concentration increased.

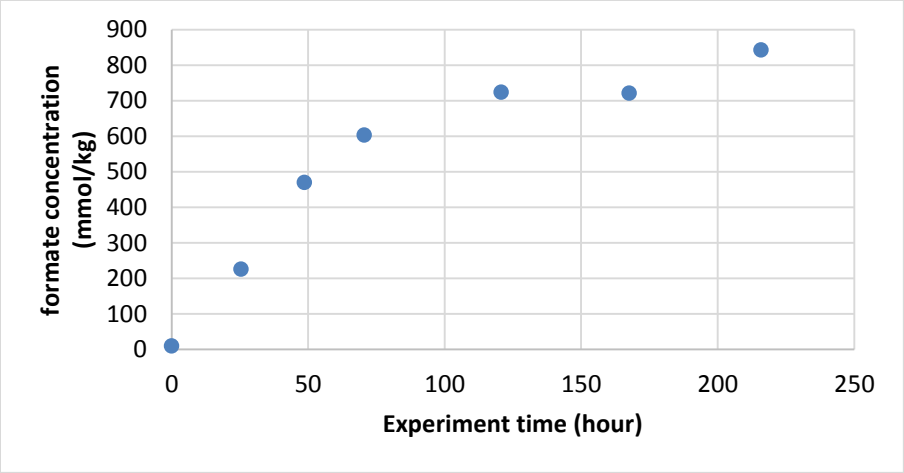

Figure 9. Oxidation product (formate) of 10 m MEA. 70 ℃, 98 kPa O2, 2 kPa CO2, 100 ml/min gas flow, 1400 rpm, 0.4 mM of Fe^{3+}, 0.2 mM Mn^{2+}, 0.1 mM Ni^{2+}, and 0.05 mM Cr^{3+}.

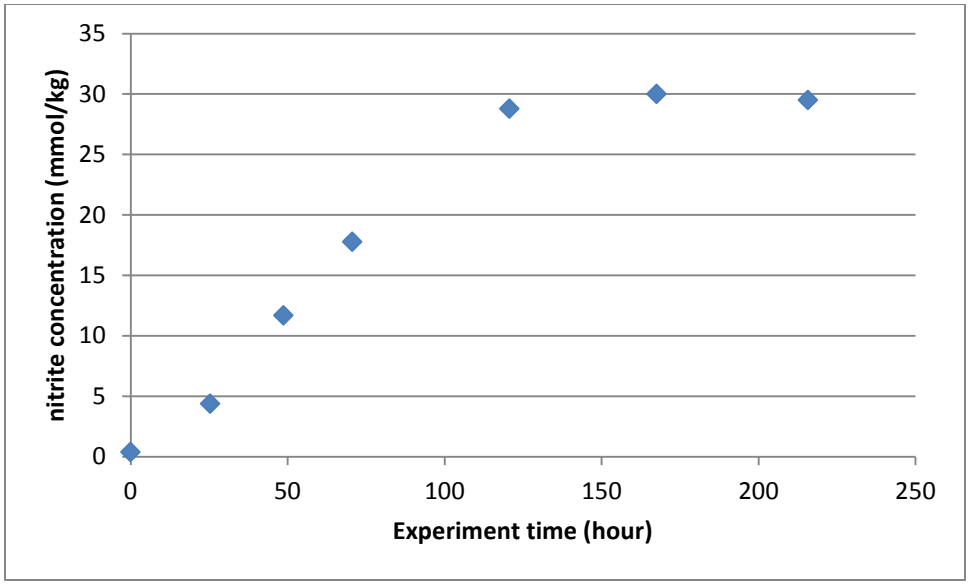

Figure 10. Oxidation product (nitrite) of 10 m MEA. 70 ℃, 98 kPa O2, 2 kPa CO2, 100 ml/min gas flow, 1400 rpm , 0.4 mM of Fe^{3+}, 0.2 mM Mn^{2+}, 0.1 mM Ni^{2+}, and 0.05 mM Cr^{3+}.

5 m 1,3-Diaminopropane (PDA)

The first trial on PDA contained 4 mM of Fe^{3+}, 2 mM Mn^{2+}, 1 mM Ni^{2+}, and 0.5 mM Cr^{3+}, 10 times the standard metals concentration (0.4 mM of Fe^{3+}, 0.2 mM Mn^{2+}, 0.1 mM Ni^{2+}, and 0.05 mM Cr^{3+}). The second trial was conducted at conditions stated in the Methodology and Scope section. In both trials, parent amine concentration fluctuated but did not change significantly over experimental period as shown in figure 10. The fluctuations were likely due to noise or water balance adjustments. A layer of foam was observed at the gas-liquid interface in the first two trials. In order to discern whether foaming hindered oxygen diffusion into the bulk solution and resulted in no degradation, a third trial was conducted with approximately 1ml of antifoam. Degradation was not observed in the third trial either, proving that the lack of degradation is not a result of hindered oxygen diffusion but a result of PDA's resistance to oxidation.

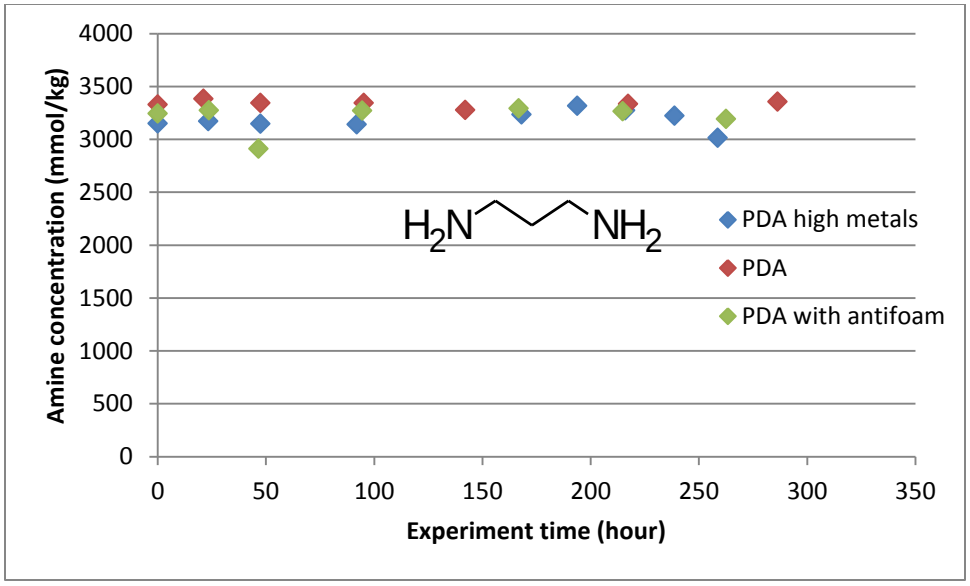

Figure 11. Oxidation of 5 m PDA. 70 ℃, 98 kPa O2, 2 kPa CO2, 100 ml/min gas flow, 1400 rpm.

Oxalate concentrations in PDA samples are not quantifiable because some data points are outside of the range of the calibration curve. The calibration curve covers 1.72-343.45 ppm oxalate, and oxalate concentration in PDA samples is either below the calibration range or small enough to be attributed to noise. Formate concentrations oscillate around 0 and some values are so small that they are outside of the calibration range (<0.94 ppm). Nitrite concentrations were nearly zero and no nitrite was produced during the experiment. The lack of oxalate and formate, both major heat stable salt oxidation products, suggests that PDA resisted oxidation in the LGF.

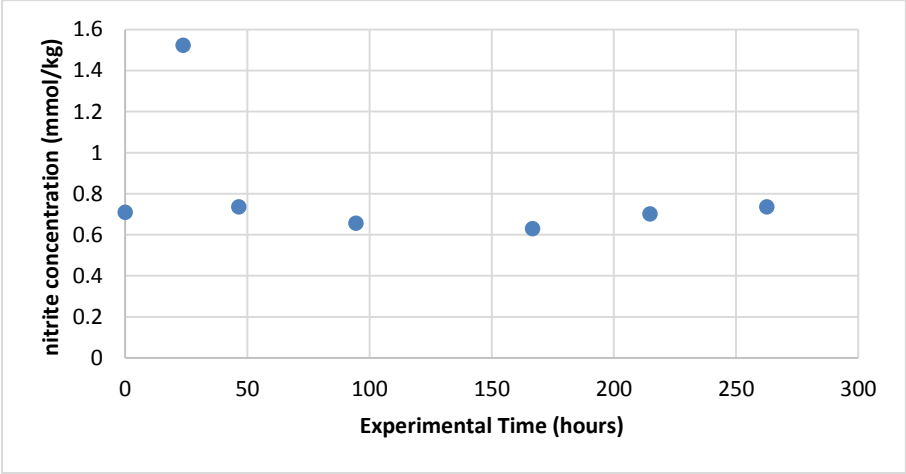

Figure 12. Oxidation product (nitrite) of 5 m PDA. 70 ℃, 98 kPa O2, 2 kPa CO2, 100 ml/min gas flow, 1400 rpm.

10 m 3-Amino-1-propanol (MPA)

MPA showed negligible degradation, approximately 10% over 260 hours. Parent amine concentration fluctuated at a constant level similar to the trends seen in PDA. Both MPA and PDA contain three carbons in the alkyl chain between the amino group and the neighboring functional group. Catalyst metals settled out of solution in PDA and MPA samples. These metals were soluble in degraded samples of other amines tested so far. Thermal degradation studies by Hatchell (Hatchell, 2015) suggested that MPA and its thermal degradation products were not corrosive, further suggesting that metals likely did not catalyze oxidative degradation due to their insolubility in PDA and MPA. Many amines that degraded significantly exhibited an induction stage. Initial degradation products may have dissolved the metals during the induction stage, allowing metals to form complexes with the amine and other species in the solution and leading to significant parent amine degradation.

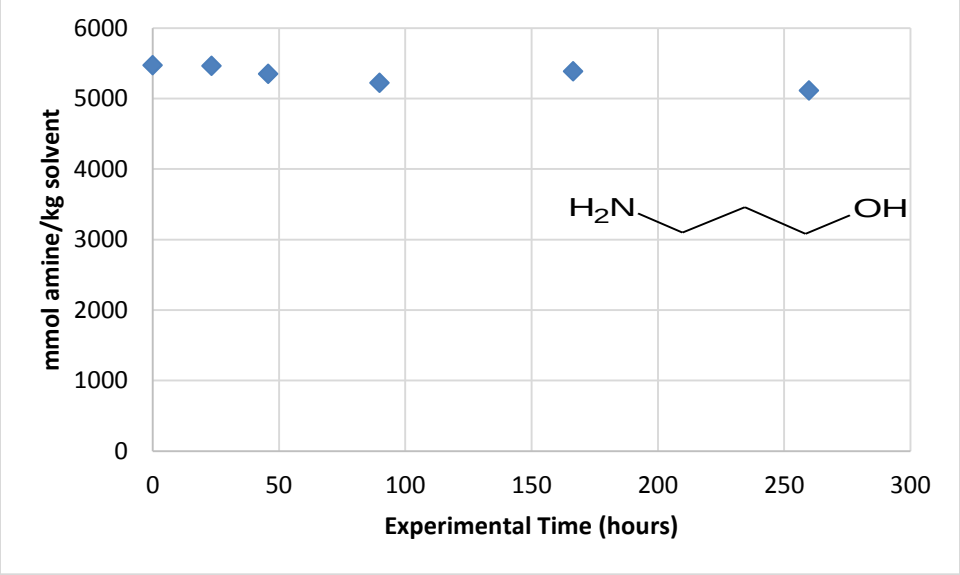

Figure 13. Oxidation of 10 m MPA. 70 ℃, 98 kPa O2, 2 kPa CO2, 100 ml/min gas flow, 1400 rpm, 0.4 mM of Fe^{3+}, 0.2 mM Mn^{2+}, 0.1 mM Ni^{2+}, and 0.05 mM Cr^{3+}.

Similar to PDA, oxalate concentrations in MPA samples was not quantifiable (<1.72 ppm). Formate concentrations are very low and relatively constant over the duration of the experiment. The absence of significant amount of degradation product supports the observation that MPA is resistant to oxidation.

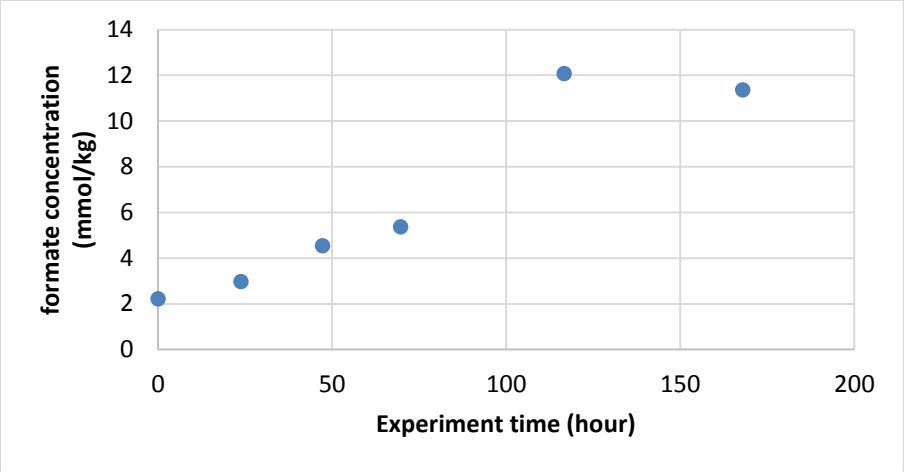

Figure 14. Oxidation product (formate) of 10 m MPA. 70 ℃, 98 kPa O2, 2 kPa CO2, 100 ml/min gas flow, 1400 rpm, 0.4 mM of Fe^{3+}, 0.2 mM Mn^{2+}, 0.1 mM Ni^{2+}, and 0.05 mM Cr^{3+}.

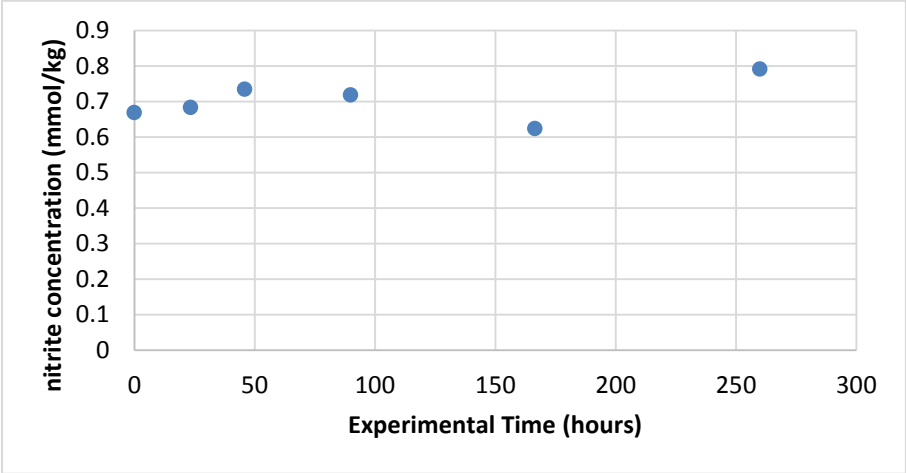

Figure 15. Oxidation product (nitrite) of 10 m MPA. 70 ℃, 98 kPa O2, 2 kPa CO2, 100 ml/min gas flow, 1400 rpm 0.4 mM of Fe^{3+}, 0.2 mM Mn^{2+}, 0.1 mM Ni^{2+}, and 0.05 mM Cr^{3+}.

5 m MEA/ 2.5 m PDA

5 m MEA/2.5 m PDA was tested to study whether PDA resistance to oxidation was due to metal insolubility or the unique chemical properties of the amine. Visual examination confirms that metals were soluble in MEA/PDA in all samples taken from the reactor. Data analysis shows no significant MEA degradation. This result suggests that PDA is resistant to oxidation due to its chemical properties, not metal insolubility.

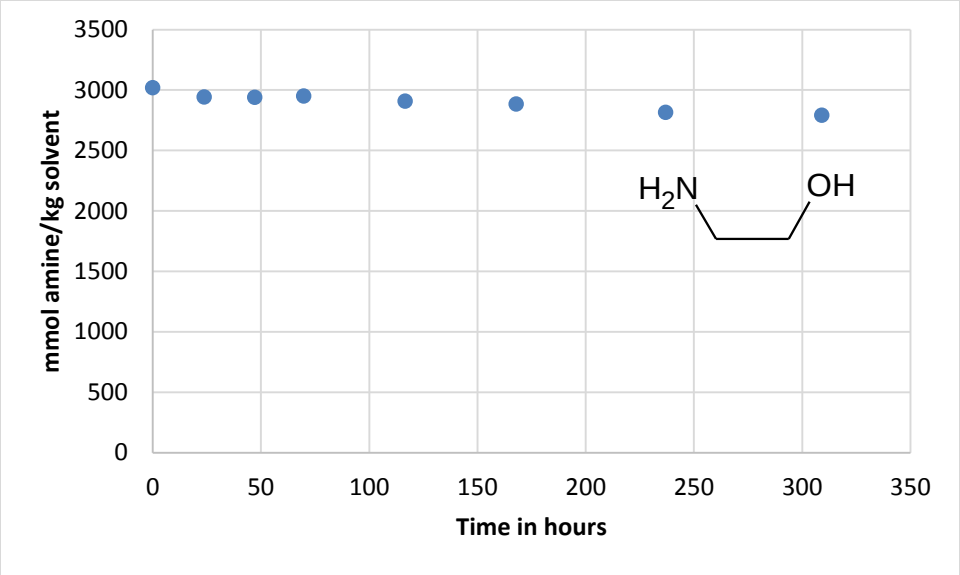

Figure 16. Oxidation of 5 m MEA/2.5 m PDA. 70 oC, 98 kPa O2, 2 kPa CO2, 100 ml/min gas flow, 1400 rpm , 0.4 mM of Fe^{3+}, 0.2 mM Mn^{2+}, 0.1 mM Ni^{2+}, and 0.05 mM Cr^{3+}.

The concentration of oxalate does increase over time in 5m MEA/2.5 m PDA, but the concentration is very low compared to that in amines that significantly degraded. This result agrees with the cation chromatography results which suggested that MEA did not degrade in this blend.

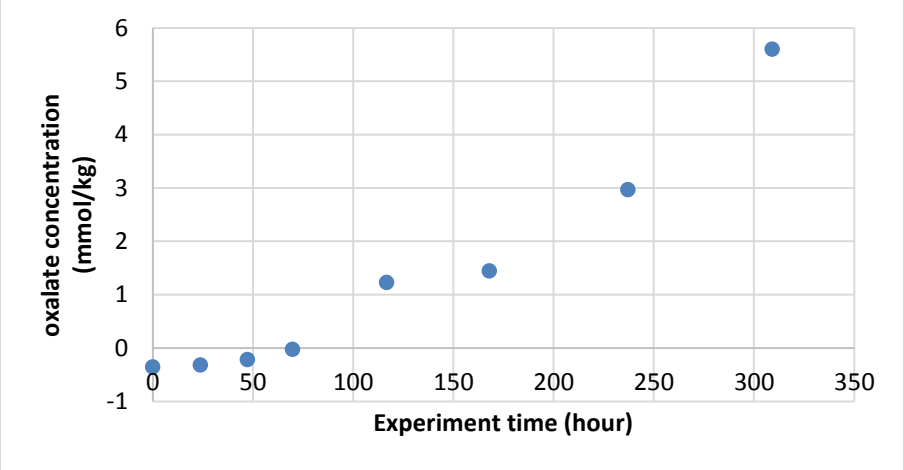

Figure 17. Oxidation product (oxalate) of 5 m MEA/2.5 m PDA. 70 oC, 98 kPa O2, 2 kPa CO2, 100 ml/min gas flow, 1400 rpm , 0.4 mM of Fe^{3+}, 0.2 mM Mn^{2+}, 0.1 mM Ni^{2+}, and 0.05 mM Cr^{3+}.

Like that seen in oxalate, formate concentration does increase over time, but the concentration is very low compared to that in amines that significantly degraded. This

observation agrees with cation chromatography results which suggested that MEA did not degrade in this blend.

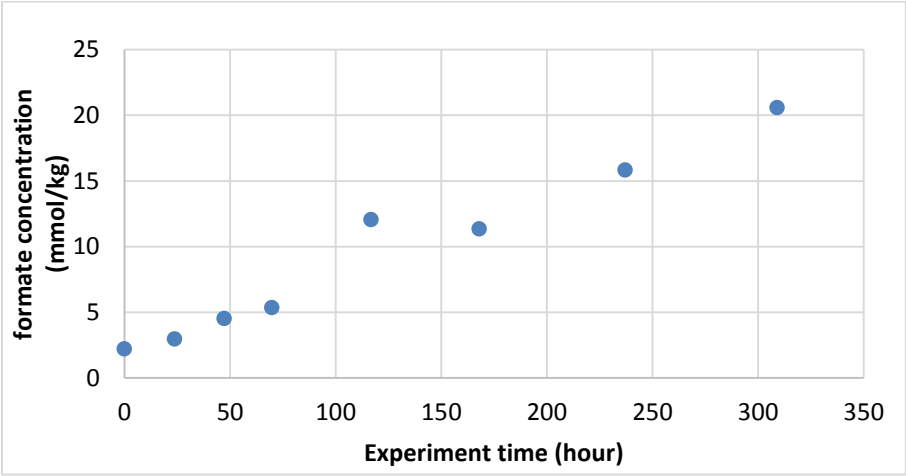

Figure 18. Oxidation product (formate) of 5 m MEA/2.5 m PDA. 70 oC, 98 kPa O2, 2 kPa CO2, 100 ml/min gas flow, 1400 rpm , 0.4 mM of Fe^{3+}, 0.2 mM Mn^{2+}, 0.1 mM Ni^{2+}, and 0.05 mM Cr^{3+}.

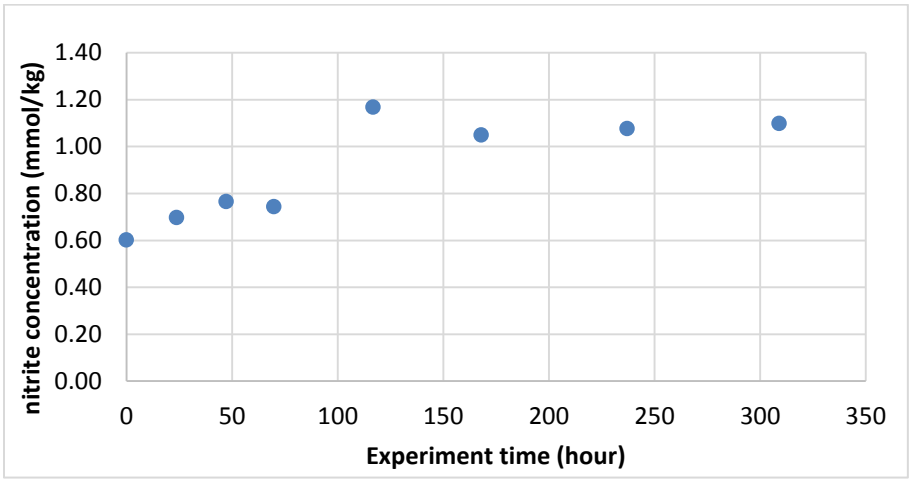

Figure 19. Oxidation product (nitrite) of 5 m MEA/2.5 m PDA. 70 oC, 98 kPa O2, 2 kPa CO2, 100 ml/min gas flow, 1400 rpm , 0.4 mM of Fe^{3+}, 0.2 mM Mn^{2+}, 0.1 mM Ni^{2+}, and 0.05 mM Cr^{3+}.

5 m Ethylenediamine (EDA)

About 80% of the parent amine EDA was lost after 286 hours. EDA concentration over time shows a linear trend, indicating that under experimental condition, degradation of EDA follows zeroth order rate law. The rate constant is 9.79 mmol/kg-hr. Results indicate that EDA is so susceptible to oxidation that the rate of oxygen diffusion into the bulk solution controls the rate of degradation.

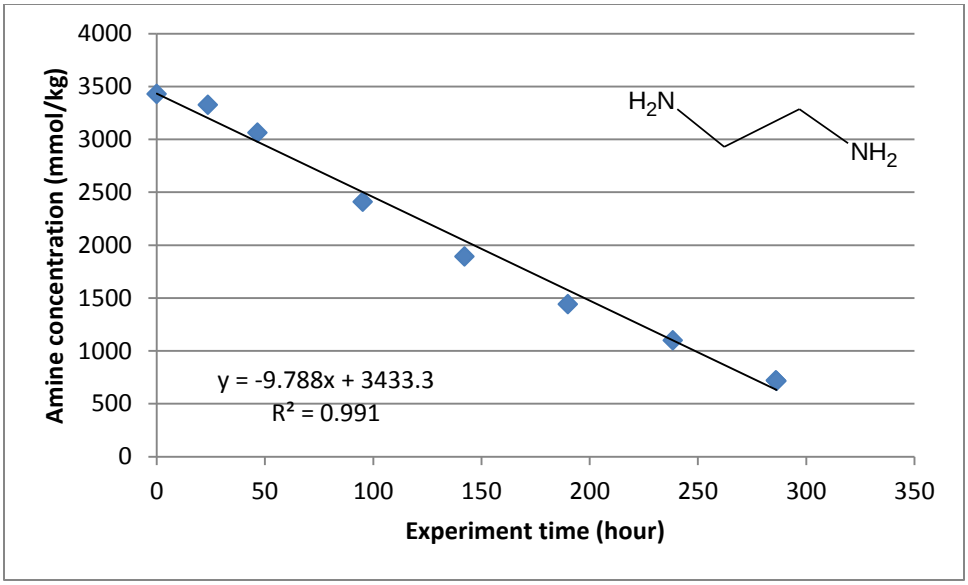

Figure 20. Oxidation of 5 m EDA. 70 ℃, 98 kPa O2, 2 kPa CO2, 100 ml/min gas flow, 1400 rpm , 0.4 mM of Fe^{3+}, 0.2 mM Mn^{2+}, 0.1 mM Ni^{2+}, and 0.05 mM Cr^{3+}.

The EDA samples cannot be found at the time of total oxalate, formate and nitrite analysis. The oxalate and formate concentration results are therefore not presented for this amine.

5 m 1,4-diaminobutane (DAB)

DAB degradation is kinetically controlled and followed first order rate law with rate constant k = 0.01/hr. About 96% of the parent amine was lost after 334 hours. DAB seems to undergo a short induction period where degradation is very slow at first but then rapidly accelerates. This result disagrees with those stated in Voice (Table A3) where he stated that DAB only degrade in the presence of Cu.

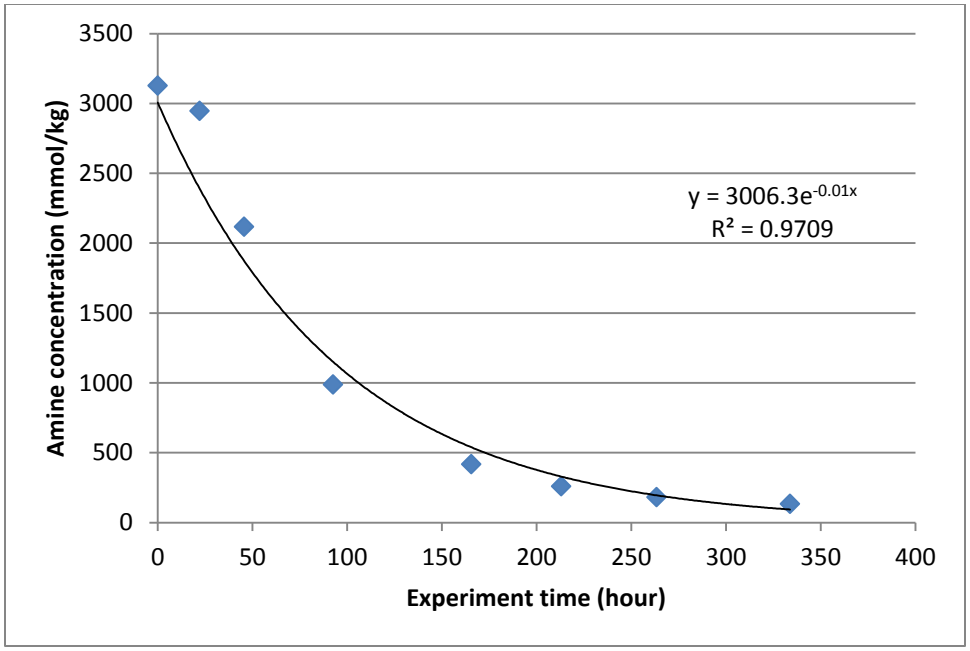

Figure 21. Oxidation of 5 m DAB. 70 ℃, 98 kPa O2, 2 kPa CO2, 100 ml/min gas flow, 1400 rpm , 0.4 mM of Fe^{3+}, 0.2 mM Mn^{2+}, 0.1 mM Ni^{2+}, and 0.05 mM Cr^{3+}.

The first 2 samples have negligible oxalate concentrations, corresponding to a very short induction period in parent amine degradation from 0 – 22 hours. However, the peak at 165 hours, the following drop and the increase in oxalate concentration after that do not follow amine loss trends.

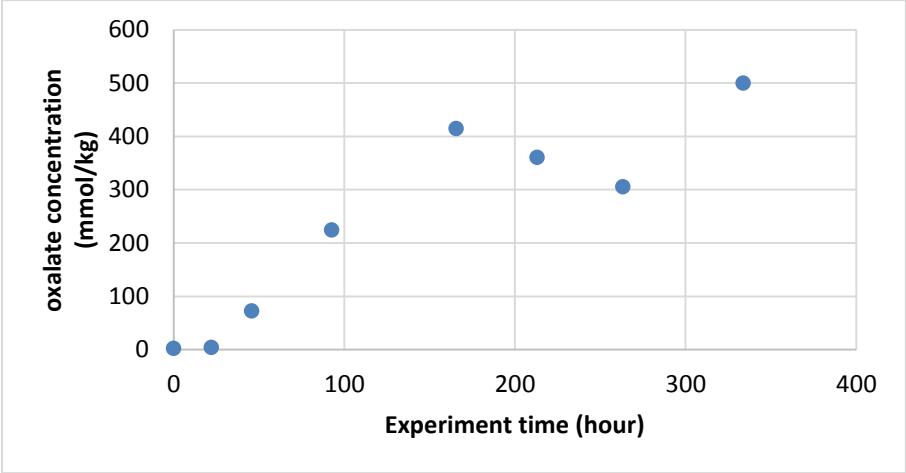

Figure 22. Oxidation product (oxalate) of 5 m DAB. 70 ℃, 98 kPa O2, 2 kPa CO2, 100 ml/min gas flow, 1400 rpm, 0.4 mM of Fe^{3+}, 0.2 mM Mn^{2+}, 0.1 mM Ni^{2+}, and 0.05 mM Cr^{3+}.

The first 2 samples have low formate concentrations, corresponding to a very short induction period in parent amine degradation from 0 – 22 hours. However, the peak

at 165 hours, the following drop and the increase in formate concentration after that do not follow amine loss trends. The same overall trend was observed in oxalate, and the concentration of oxalate and formate are very similar in each sample.

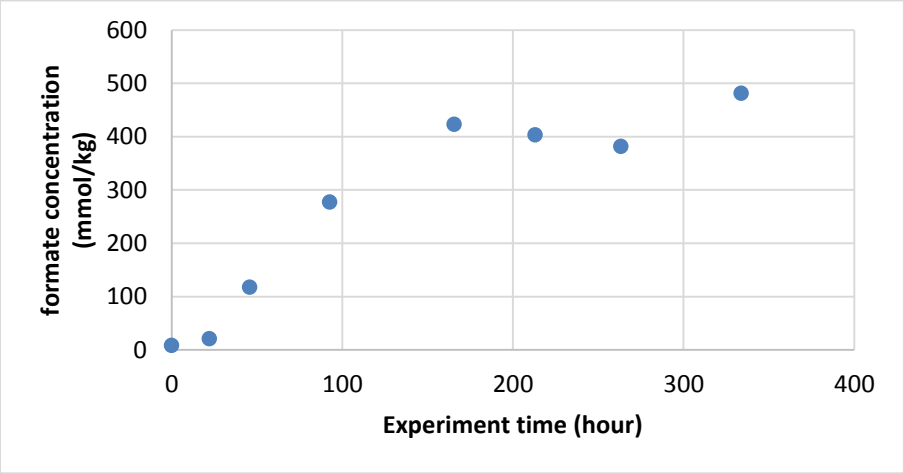

Figure 23. Oxidation product (formate) of 5 m DAB. 70 ℃, 98 kPa O2, 2 kPa CO2, 100 ml/min gas flow, 1400 rpm , 0.4 mM of Fe^{3+}, 0.2 mM Mn^{2+}, 0.1 mM Ni^{2+}, and 0.05 mM Cr^{3+}.

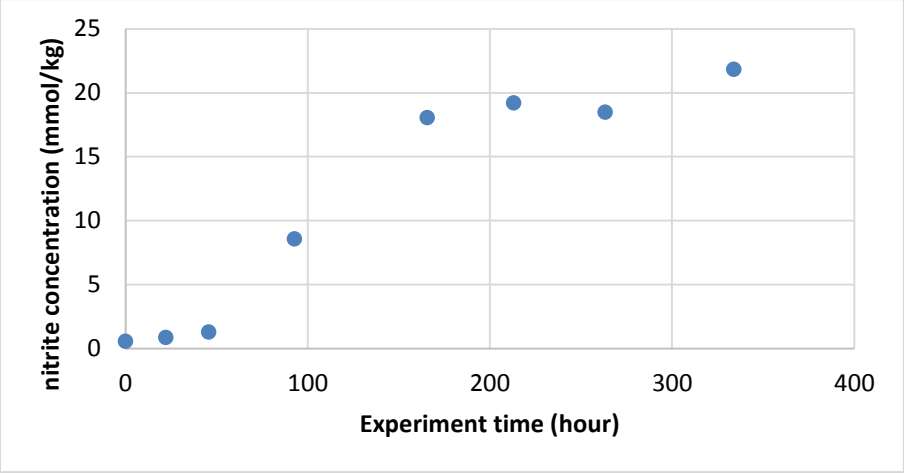

Figure 24. Oxidation product (nitrite) of 5 m DAB. 70 ℃, 98 kPa O2, 2 kPa CO2, 100 ml/min gas flow, 1400 rpm , 0.4 mM of Fe^{3+}, 0.2 mM Mn^{2+}, 0.1 mM Ni^{2+}, and 0.05 mM Cr^{3+}.

5 m Hexamethylenediamine (HMDA)

An induction period similar to that observed in DAB was also present in HMDA degradation. Only the last four data points were used to calculate the rate of degradation. HMDA degradation is kinetically controlled following first order rate law with rate constant k = 0.01/hr. About 80% of the HMDA was lost to degradation.

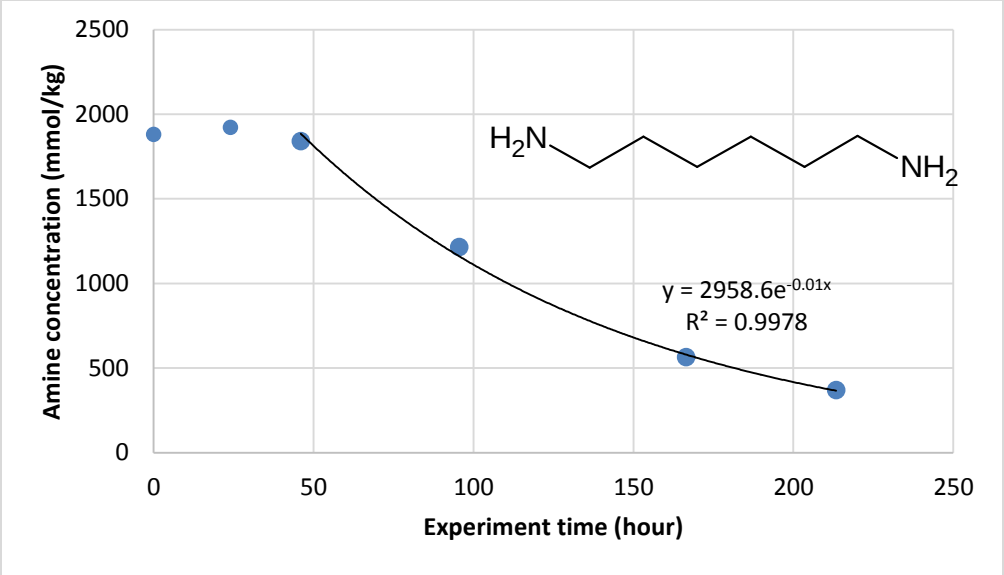

Figure 25. Oxidation of 5 m HMDA. 70 ℃, 98 kPa O2, 2 kPa CO2, 100 ml/min gas flow, 1400 rpm , 0.4 mM of Fe^{3+}, 0.2 mM Mn^{2+}, 0.1 mM Ni^{2+}, and 0.05 mM Cr^{3+}.

The concentration of oxalate concentration is very low initially, corresponding to the induction period seen in cation chromatography results. Oxalate production started at the same time as parent amine degradation. While parent amine degradation followed first order rate law, oxalate formation increased linearly.

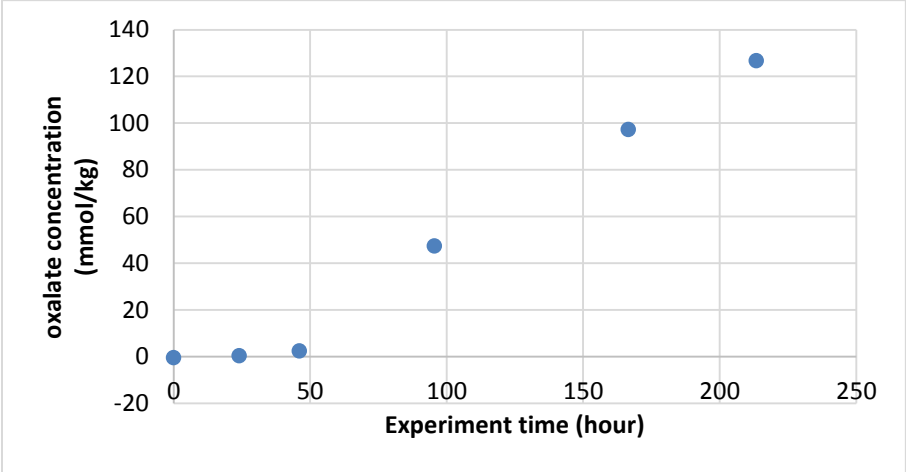

Figure 26. Oxidation product (oxalate) of 5 m HMDA. 70 ℃, 98 kPa O2, 2 kPa CO2, 100 ml/min gas flow, 1400 rpm , 0.4 mM of Fe^{3+}, 0.2 mM Mn^{2+}, 0.1 mM Ni^{2+}, and 0.05 mM Cr^{3+}.

The formate concentrations in HMDA samples follow similar trends as oxalate concentrations. Samples collected during the induction period have very low formate concentrations, which increased as soon as degradation rapidly accelerates.

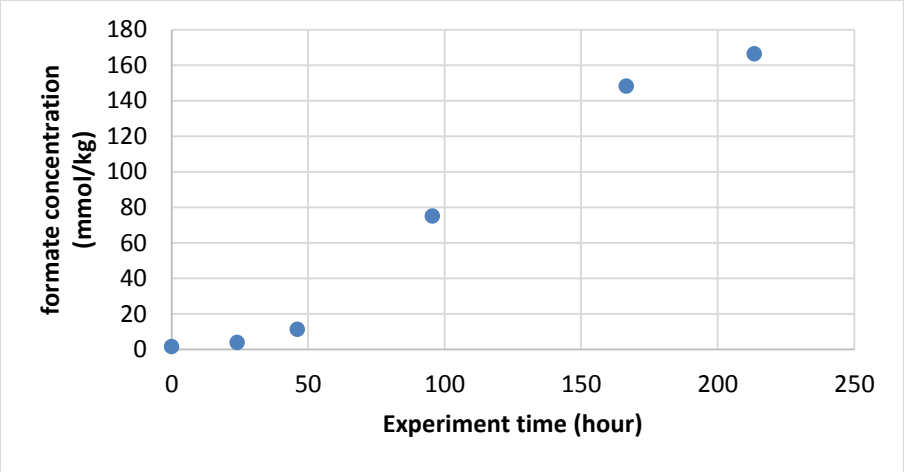

Figure 27. Oxidation product (formate) of 5 m HMDA. 70 ℃, 98 kPa O2, 2 kPa CO2, 100 ml/min gas flow, 1400 rpm , 0.4 mM of Fe^{3+}, 0.2 mM Mn^{2+}, 0.1 mM Ni^{2+}, and 0.05 mM Cr^{3+}.

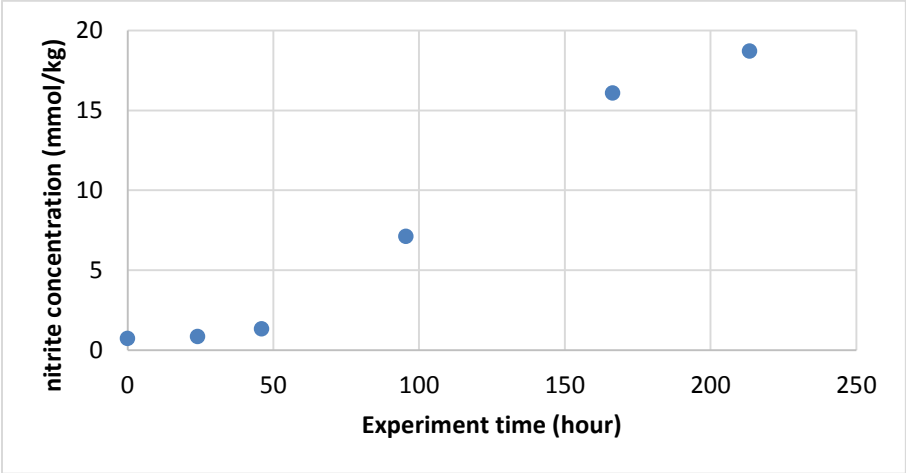

Figure 28. Oxidation product (nitrite) of 5 m HMDA. 70 ℃, 98 kPa O2, 2 kPa CO2, 100 ml/min gas flow, 1400 rpm , 0.4 mM of Fe^{3+}, 0.2 mM Mn^{2+}, 0.1 mM Ni^{2+}, and 0.05 mM Cr^{3+}.

5 m Bis(2-aminoethyl) Ether (Jeffamine®)

Degradation of Jeffamine® followed first order rate law initially with a rate constant 0.023/hr using the first four data points. The rate constant is much higher than that of the other amines tested. About 90% of the initial amount of amine was lost to degradation. There is no observable induction period, and degradation reached equilibrium after approximately 100 hours.

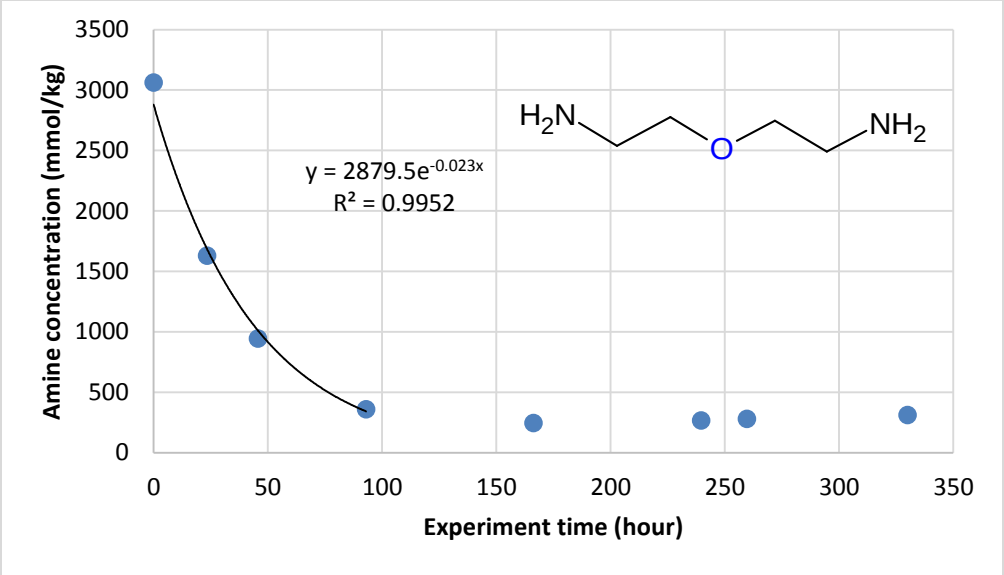

Figure 29. Oxidation of 5 m Jeffamine®. 70 ℃, 98 kPa O2, 2 kPa CO2, 100 ml/min gas flow, 1400 rpm , 0.4 mM of Fe^{3+}, 0.2 mM Mn^{2+}, 0.1 mM Ni^{2+}, and 0.05 mM Cr^{3+}.

Oxalate concentration is much higher in degraded Jeffamine® samples than in any other degraded amine samples. The initial linear increase in oxalate concentration corresponds to first order parent amine degradation until approximately 100 hours. When parent amine degradation reached equilibrium, oxalate concentration plateaued, then continued to increase starting at 200 hours but soon reached another equilibrium. The presence of two equilibrium concentrations is not observed in other amines. Oxalate concentrations after approximately 200 hours do not correspond consistently with parent amine degradation trends.

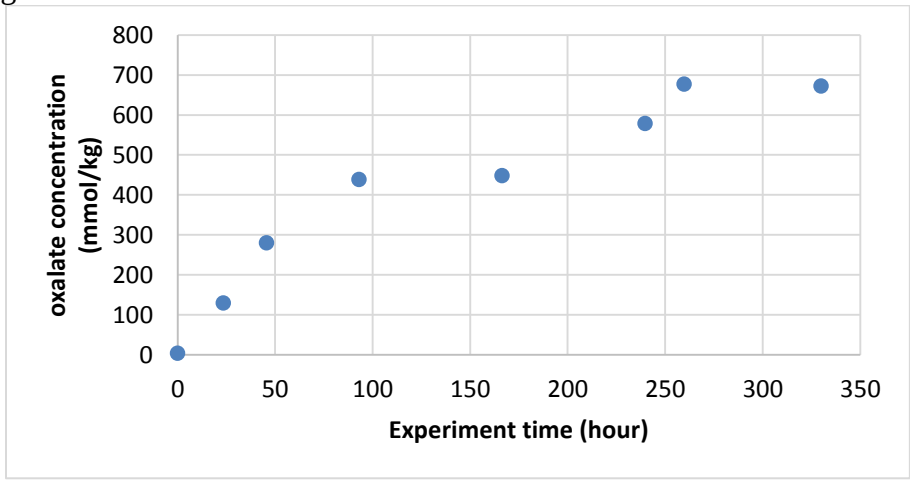

Figure 30. Oxidation product (oxalate) of 5 m Jeffamine®. 70 ℃, 98 kPa O2, 2 kPa CO2, 100 ml/min gas flow, 1400 rpm , 0.4 mM of Fe^{3+}, 0.2 mM Mn^{2+}, 0.1 mM Ni^{2+}, and 0.05 mM Cr^{3+}.

Formate concentration is much higher in degraded Jeffamine® samples than in any other degraded amine samples, same as that seen in oxalate analysis. Formate production corresponds with parent amine degradation until formate concentration started to increase and reached another equilibrium concentration after the first plateau. Formate production trend after approximately 200 hours does not correspond consistently with parent amine degradation trends.

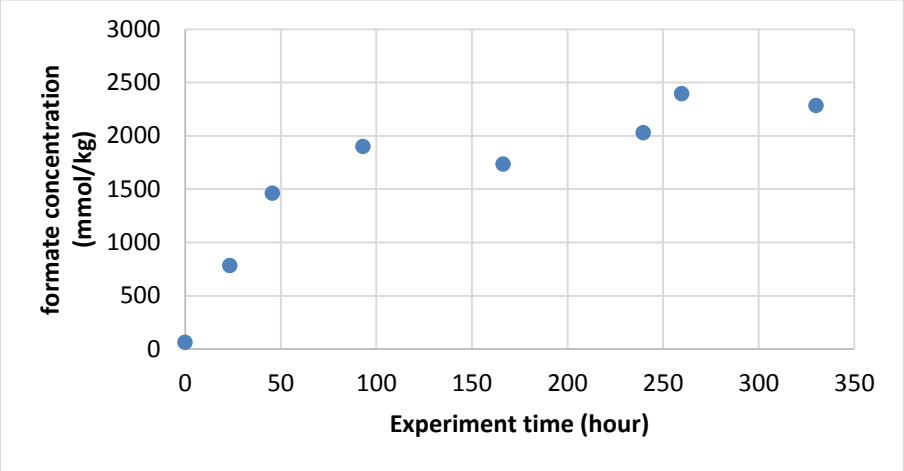

Figure 31. Oxidation product (formate) of 5 m Jeffamine®. 70 ℃, 98 kPa O2, 2 kPa CO2, 100 ml/min gas flow, 1400 rpm, 0.4 mM of Fe^{3+}, 0.2 mM Mn^{2+}, 0.1 mM Ni^{2+}, and 0.05 mM Cr^{3+}.

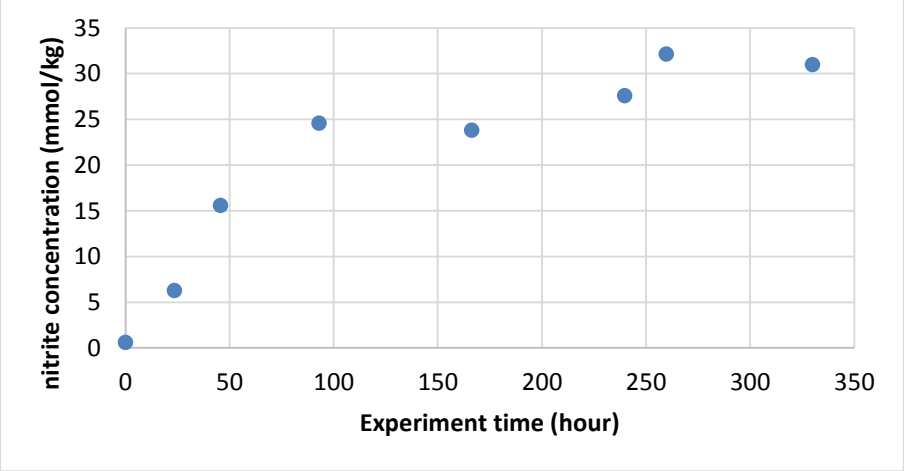

Figure 32. Oxidation product (nitrite) of 5 m Jeffamine®. 70 ℃, 98 kPa O2, 2 kPa CO2, 100 ml/min gas flow, 1400 rpm, 0.4 mM of Fe^{3+}, 0.2 mM Mn^{2+}, 0.1 mM Ni^{2+}, and 0.05 mM Cr^{3+}.

10 m Diglycolamine® (DGA®)

DGA degradation followed first order rate law with rate constant k = 0.011/hr. The fit excluded the last data point in order to obtain an acceptable R^2 value. There is no observable induction stage. Degradation is kinetically controlled and about 80% of the parent amine was lost to degradation.

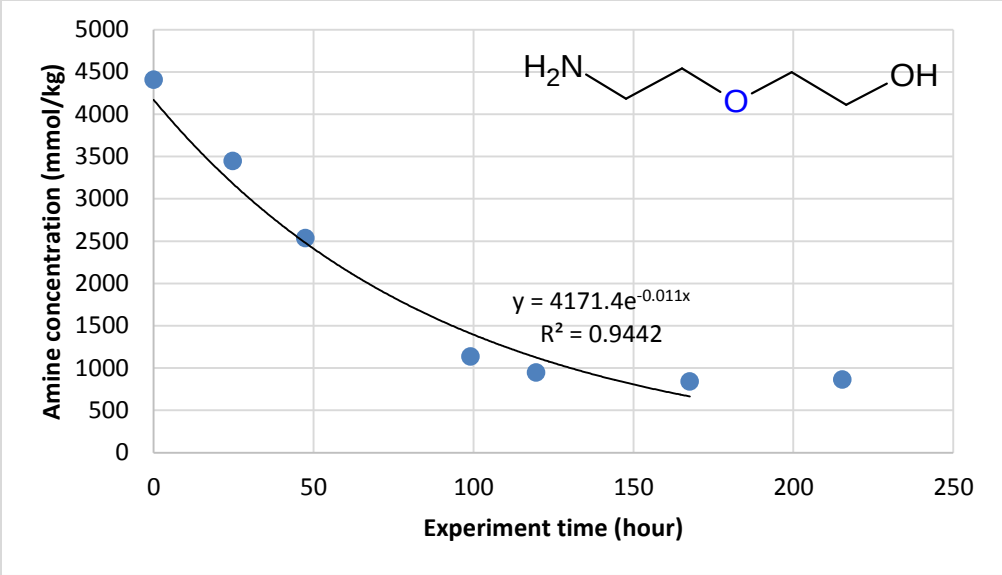

Figure 33. Oxidation of 10 m DGA®. 70 ℃, 98 kPa O2, 2 kPa CO2, 100 ml/min gas flow, 1400 rpm, 0.4 mM of Fe^{3+}, 0.2 mM Mn^{2+}, 0.1 mM Ni^{2+}, and 0.05 mM Cr^{3+}.

Oxalate formation followed parent amine degradation trends fairly consistently. As parent amine degraded by first order rate law, oxalate formation steadily increased, following a somewhat linear trend although the rate of formation seemed to be different between 0 – 50 hours and 120 – 215 hours.

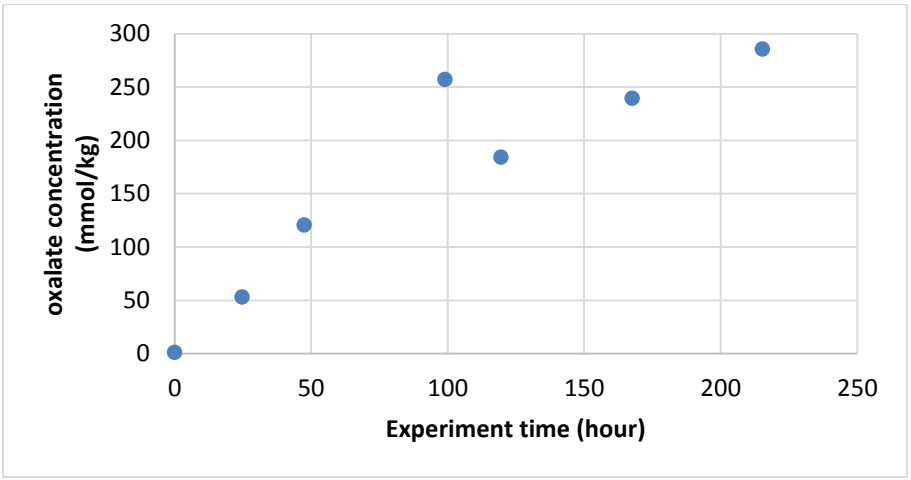

Figure 34. Oxidation product (oxalate) of 10 m DGA®. 70 ℃, 98 kPa O2, 2 kPa CO2, 100 ml/min gas flow, 1400 rpm, 0.4 mM of Fe^{3+}, 0.2 mM Mn^{2+}, 0.1 mM Ni^{2+}, and 0.05 mM Cr^{3+}.

Formate concentration is much higher than oxalate concentration in degraded DGA samples. Formate production followed parent amine degradation trends very consistently. When parent amine degradation reached equilibrium, formate concentration stopped increasing and became constant.

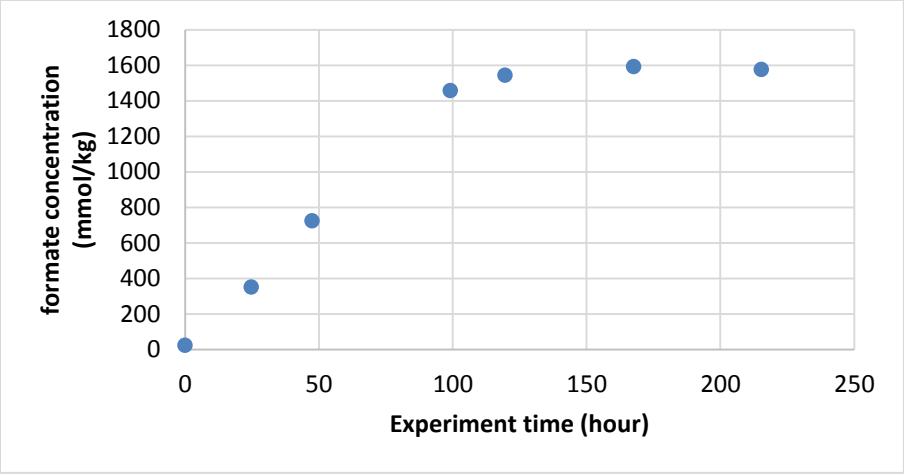

Figure 35. Oxidation product (formate) of 10 m DGA®. 70 ℃, 98 kPa O2, 2 kPa CO2, 100 ml/min gas flow, 1400 rpm, 0.4 mM of Fe^{3+}, 0.2 mM Mn^{2+}, 0.1 mM Ni^{2+}, and 0.05 mM Cr^{3+}.

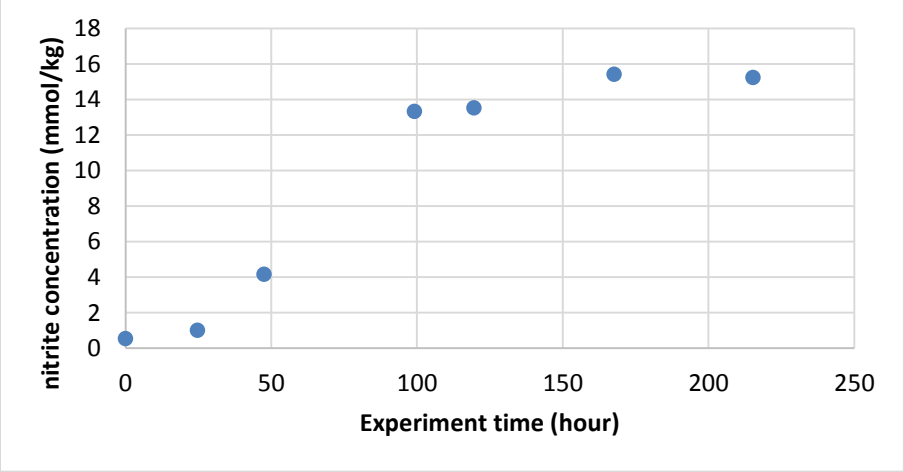

Figure 36. Oxidation product (nitrite) of 10 m DGA®. 70 ℃, 98 kPa O2, 2 kPa CO2, 100 ml/min gas flow, 1400 rpm, 0.4 mM of Fe^{3+}, 0.2 mM Mn^{2+}, 0.1 mM Ni^{2+}, and 0.05 mM Cr^{3+}.

5 m Diethanolamine (DEA)

The first five points were used to construct a second order rate law fit and points after degradation reached equilibrium were not included in the fit. DEA degradation followed 2nd order rate law with rate constant $3*10^{-6}$ $(mmol/kg\text{-}hr)^{-1}$ and 69% of the parent amine was lost by the end of the experiment.

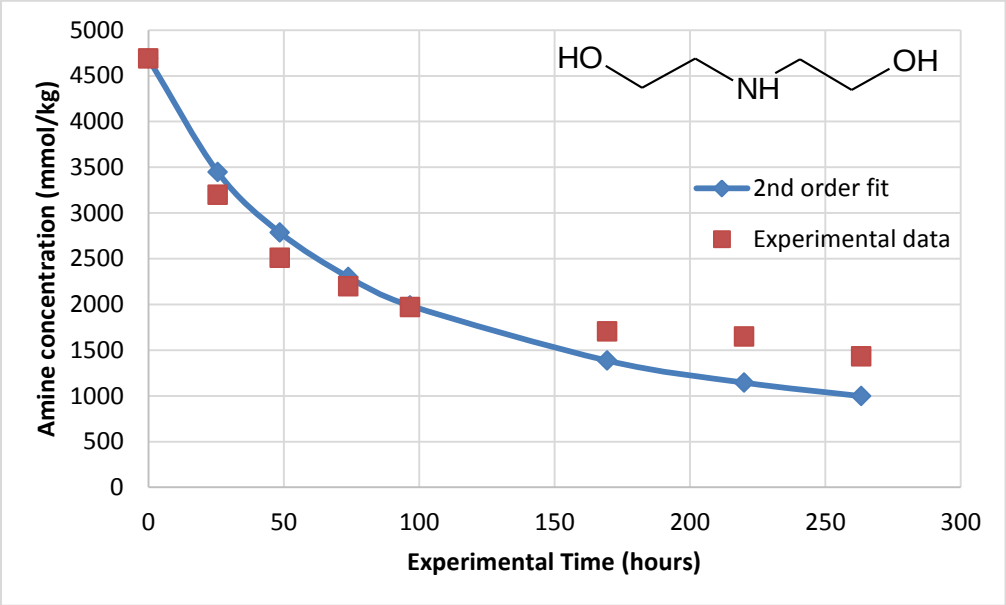

Figure 37. Oxidation of 5 m DEA. 70 ℃, 98 kPa O2, 2 kPa CO2, 100 ml/min gas flow, 1400 rpm, 0.4 mM of Fe^{3+}, 0.2 mM Mn^{2+}, 0.1 mM Ni^{2+}, and 0.05 mM Cr^{3+}.

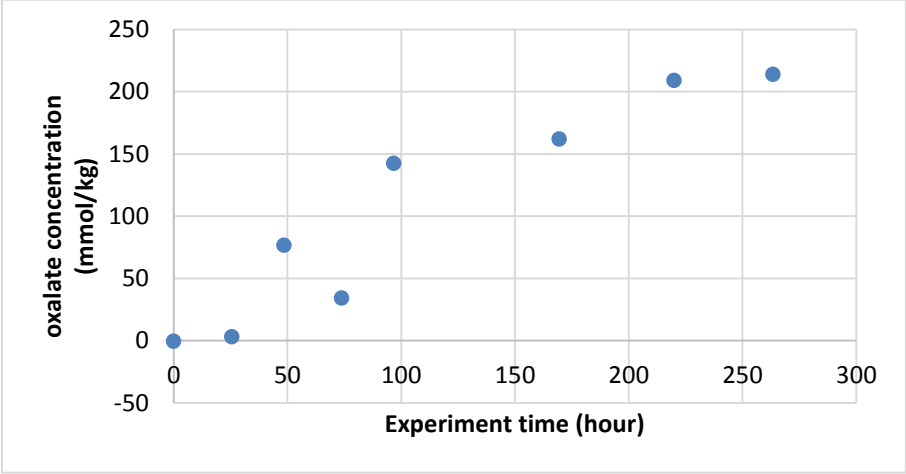

Figure 38. Oxidation product (oxalate) of 5 m DEA. 70 ℃, 98 kPa O2, 2 kPa CO2, 100 ml/min gas flow, 1400 rpm, 0.4 mM of Fe^{3+}, 0.2 mM Mn^{2+}, 0.1 mM Ni^{2+}, and 0.05 mM Cr^{3+}.

Formate concentration is much higher compared to oxalate concentration in degraded DEA samples. Parent amine degradation corresponds to the trend of formate production. A linear fit of the trend returns an R^2 of 0.9712, showing that just like oxalate, formate production may be linear in some cases.

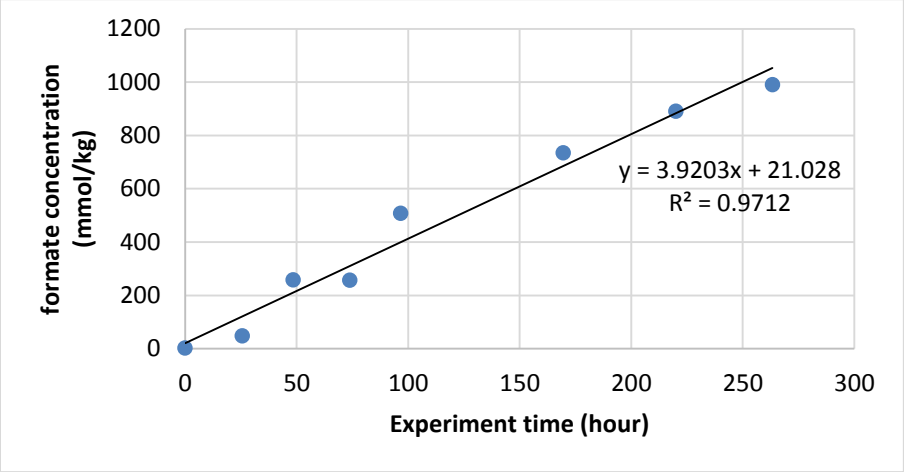

Figure 39. Oxidation product (formate) of 5 m DEA. 70 ℃, 98 kPa O2, 2 kPa CO2, 100 ml/min gas flow, 1400 rpm, 0.4 mM of Fe^{3+}, 0.2 mM Mn^{2+}, 0.1 mM Ni^{2+}, and 0.05 mM Cr^{3+}.

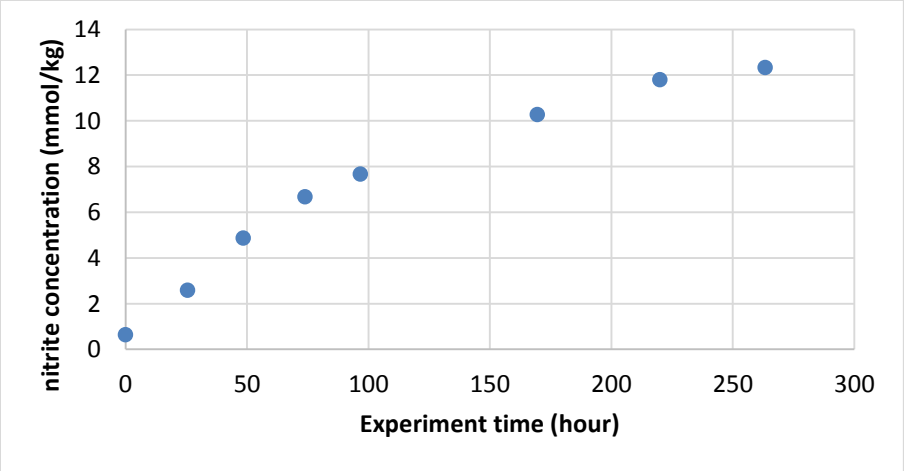

Figure 40. Oxidation product (nitrite) of 5 m DEA. 70 ℃, 98 kPa O2, 2 kPa CO2, 100 ml/min gas flow, 1400 rpm, 0.4 mM of Fe^{3+}, 0.2 mM Mn^{2+}, 0.1 mM Ni^{2+}, and 0.05 mM Cr^{3+}.

5 m Methylaminoethanol (MAE)

The degradation of MAE followed 2nd order rate law with rate constant $9*10^{-7}$ $(mmol/kg\text{-}hr)^{-1}$. About 63% of the amine was lost by the end of the experimental period.

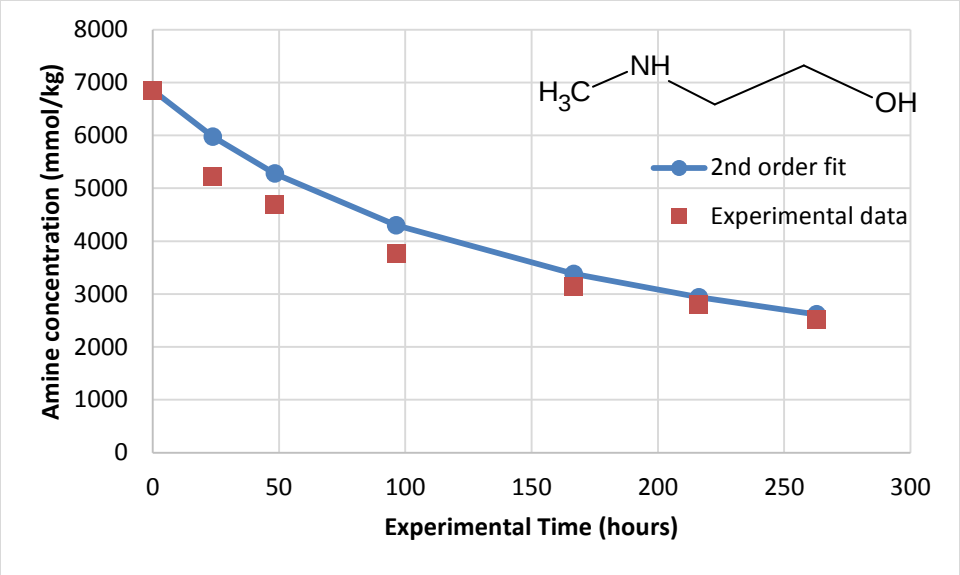

Figure 41. Oxidation of 5 m MAE. 70 ℃, 98 kPa O2, 2 kPa CO2, 100 ml/min gas flow, 1400 rpm, 0.4 mM of Fe^{3+}, 0.2 mM Mn^{2+}, 0.1 mM Ni^{2+}, and 0.05 mM Cr^{3+}.

Oxalate concentration is substantial in degraded MAE samples and increases with time. The rate of formation is nearly linear initially, but seems to slowly approach equilibrium if the trend is extended.

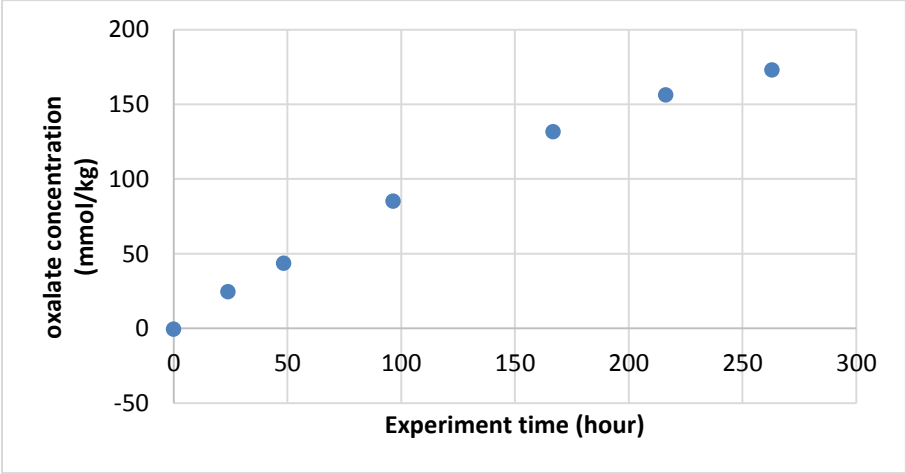

Figure 42. Oxidation product (oxalate) of 5 m MAE. 70 ℃, 98 kPa O2, 2 kPa CO2, 100 ml/min gas flow, 1400 rpm, 0.4 mM of Fe^{3+}, 0.2 mM Mn^{2+}, 0.1 mM Ni^{2+}, and 0.05 mM Cr^{3+}.

Formate concentration is greater than oxalate concentration in degraded MAE samples and increases with time as degradation takes place. The rate of formate production is very linear but the trend does tend toward equilibrium near the end. For some amines, formate production follows a linear trend.

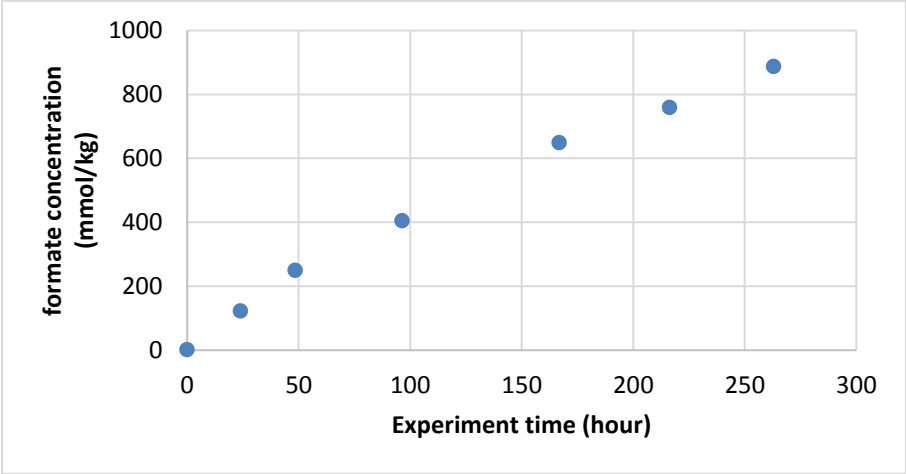

Figure 43. Oxidation product (formate) of 5 m MAE. 70 ℃, 98 kPa O2, 2 kPa CO2, 100 ml/min gas flow, 1400 rpm, 0.4 mM of Fe^{3+}, 0.2 mM Mn^{2+}, 0.1 mM Ni^{2+}, and 0.05 mM Cr^{3+}.

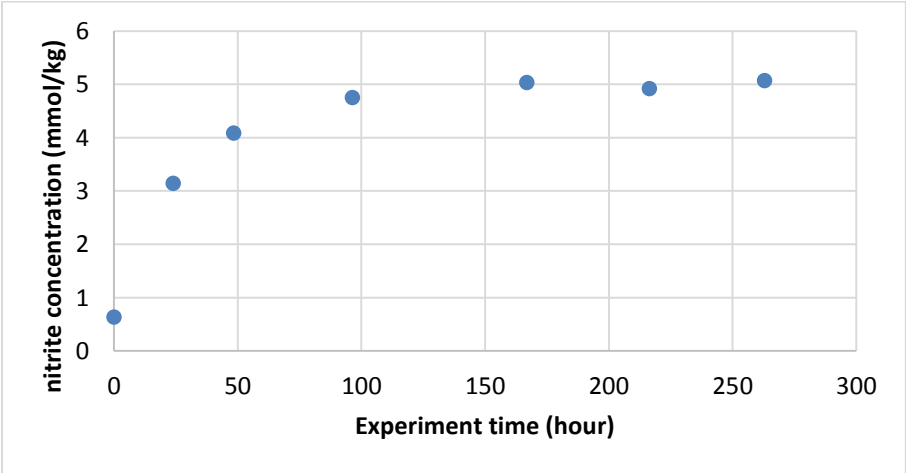

Figure 44. Oxidation product (nitrite) of 5 m MAE. 70 ℃, 98 kPa O2, 2 kPa CO2, 100 ml/min gas flow, 1400 rpm, 0.4 mM of Fe^{3+}, 0.2 mM Mn^{2+}, 0.1 mM Ni^{2+}, and 0.05 mM Cr^{3+}.

5 m 3-(Methylamino)propylamine (MAPA)

MAPA degradation is kinetically controlled at experimental conditions and the rate constant k is approximately 0.016 hr^{-1}. In the last sample of MAPA, cation chromatography results does not show any peak, indicating that MAPA is almost completely consumed by the end of the experiment (169 hours). Previous work by Voice reported that MAPA degrades at a rate higher than MEA, the base comparison amine for most studies. MAPA showed similar or greater amount of volatile degradation products

compared to MEA at similar conditions and the mechanism for oxidation may involve metal-amine complexes (Voice, 2013).

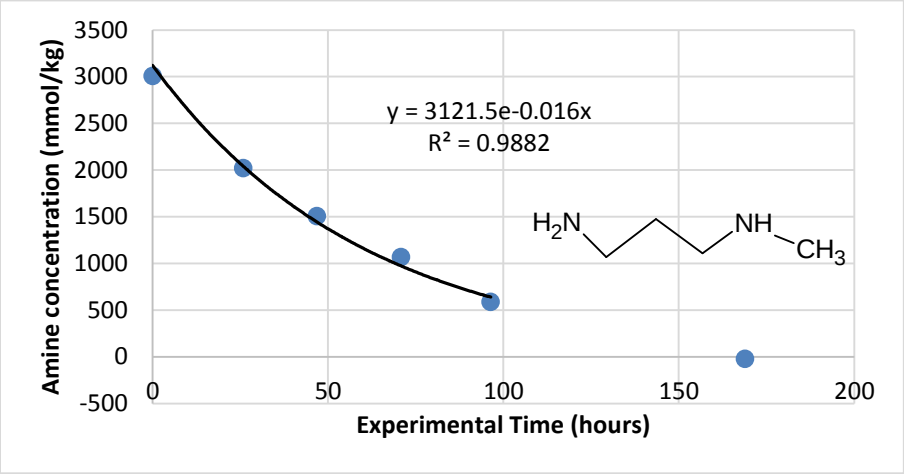

Figure 45. Oxidation of 5 m MAPA. 70 ℃, 98 kPa O2, 2 kPa CO2, 100 ml/min gas flow, 1400 rpm, 0.4 mM of Fe^{3+}, 0.2 mM Mn^{2+}, 0.1 mM Ni^{2+}, and 0.05 mM Cr^{3+}.

The rate of oxalate formation is very low initially despite significant MAPA degradation. Oxalate concentration rapidly increased between approximately 100 – 170 hours, and during this time, degradation continued until all parent amine was consumed at the end of the experiment. Oxalate formation of MAPA suggested that it is difficult to correlate oxalate formation rate directly to parent amine degradation rate because while MAPA steadily degraded throughout the experiment, oxalate formation rate started slow and rapidly accelerated near the end.

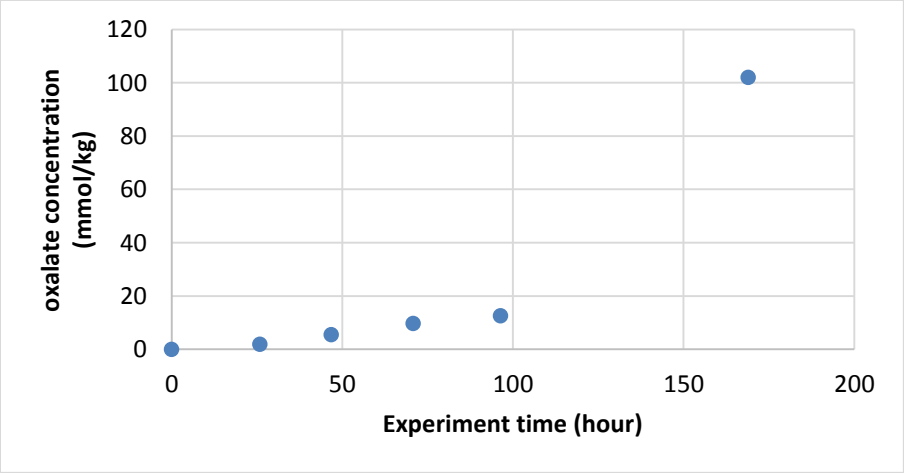

Figure 46. Oxidation product (oxalate) of 5 m MAPA. 70 ℃, 98 kPa O2, 2 kPa CO2, 100 ml/min gas flow, 1400 rpm, 0.4 mM of Fe^{3+}, 0.2 mM Mn^{2+}, 0.1 mM Ni^{2+}, and 0.05 mM Cr^{3+}.

Formate production trend is very similar to oxalate production trend in degraded MAPA samples. While MAPA steadily degraded throughout the experiment, formate production rate started slow and rapidly accelerated near the end between approximately 100 – 170 hours when all parent amines were consumed.

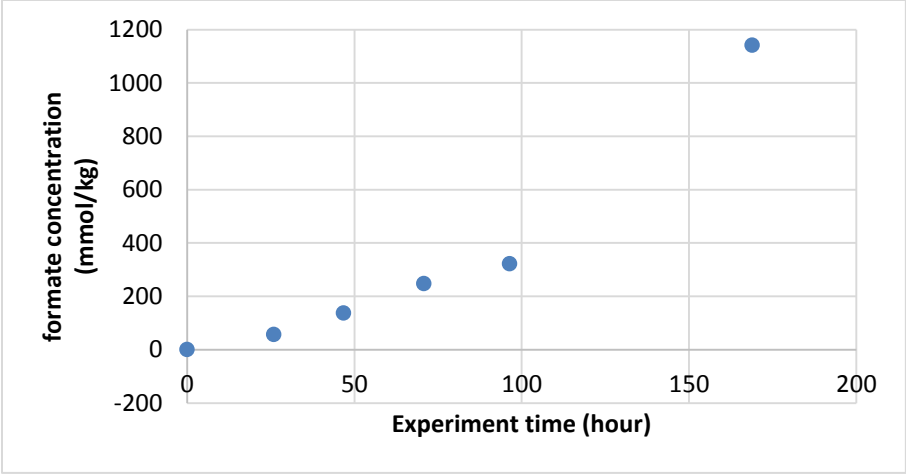

Figure 47. Oxidation product (formate) of 5 m MAPA. 70 ℃, 98 kPa O2, 2 kPa CO2, 100 ml/min gas flow, 1400 rpm, 0.4 mM of Fe^{3+}, 0.2 mM Mn^{2+}, 0.1 mM Ni^{2+}, and 0.05 mM Cr^{3+}.

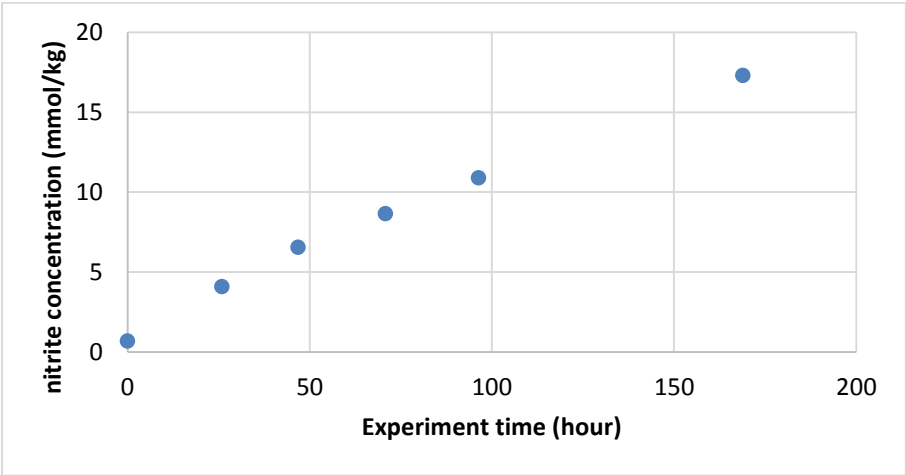

Figure 48. Oxidation product (nitrite) of 5 m MAPA. 70 ℃, 98 kPa O2, 2 kPa CO2, 100 ml/min gas flow, 1400 rpm, 0.4 mM of Fe^{3+}, 0.2 mM Mn^{2+}, 0.1 mM Ni^{2+}, and 0.05 mM Cr^{3+}.

3.33 m 2-Dimethylaminoethanol/3.33 m piperazine (DMAE/PZ)

DMAE/PZ blend with loading 0.25 mol CO_2/mol alkalinity seemed to follow first order rate law with k_0=0.01 hr^{-1} in the beginning and reached equilibrium after approximately 50 hours. PZ was added as a rate promoter for CO_2 absorption. Initial DMAE degradation could have been kinetically controlled. Parent amine loss was approximately 40% by the end of experiment. Previous works stated tertiary amines show resistance to degradation, but DMAE loss in this case is greater than expected. After analysis with cation chromatography, researcher realized the experimental solution contained significant amount of MAE that's mistakenly used to prepare the stock solution. Data is still included in this report, but the concentration of DMAE and exact loading are different from intended values. Concentration of MAE remained largely constant in all samples, implying MAE showed negligible degradation. This observation confirmed Voice's conclusion that tertiary amines were able to protect primary and secondary amines from oxidation (Voice, 2013).

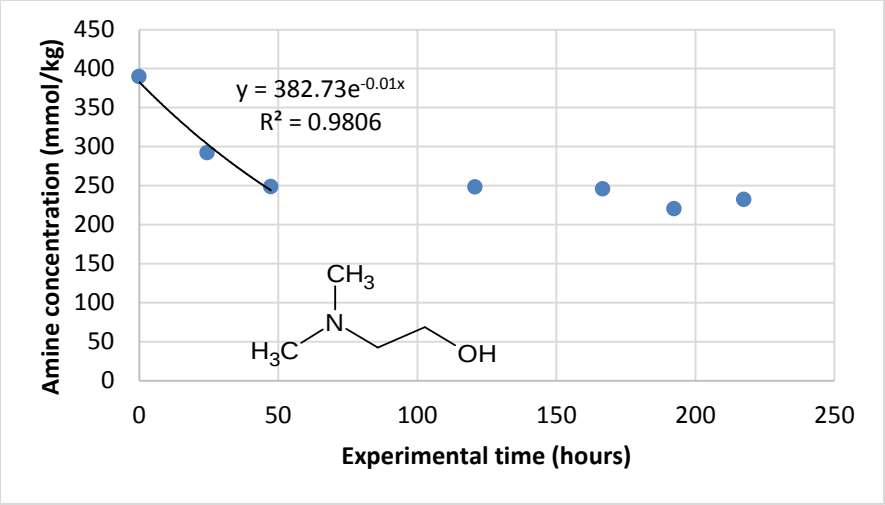

Figure 49. Oxidation of 3.33 m DMAE/3.33 m PZ. Conditions: unknown loading, 70 ℃, 98 kPa O2, 2 kPa CO2, 100 ml/min gas flow, 1400 rpm , 0.4 mM of Fe^{3+}, 0.2 mM Mn^{2+}, 0.1 mM Ni^{2+}, and 0.05 mM Cr^{3+}.

Another trial of DMAE/PZ was conducted again with the correct setup. This time, slight degradation was observed. Voice's work concluded that tertiary amines resist oxidation. However, figure 42 shows that amine concentration seems to be linearly decreasing over time. Linear loss trend usually correlates to a zeroth order rate law, meaning that rate of oxygen diffusion into the bulk solution controls rate of degradation. However, given the expectation that significant degradation is unlikely, diffusion controlled regime does not seem plausible. Another possibility is that water balance was not well-maintained over experimental period. A higher concentration of water could lower the relative concentration of amine at the end of the experiment and lead to a false degradation trend.

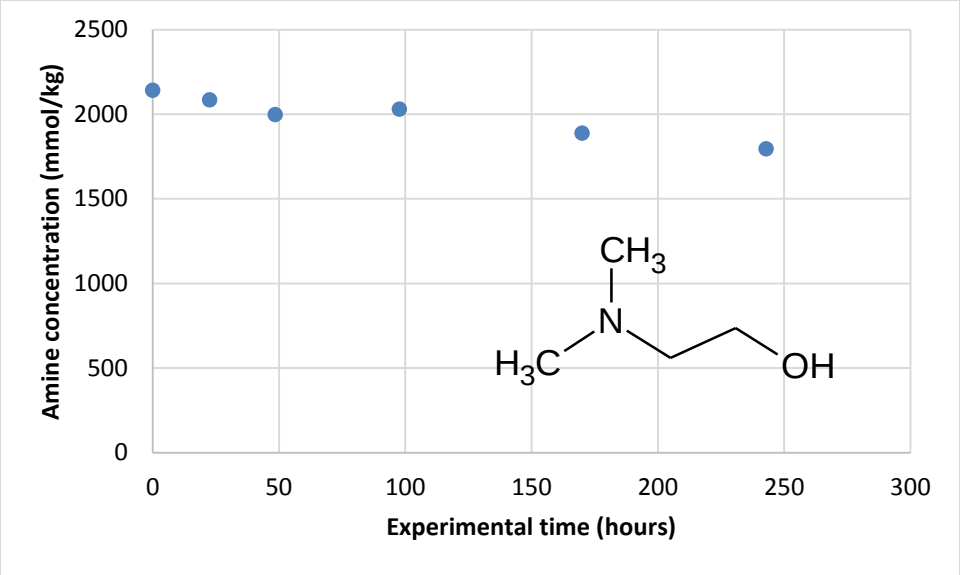

Figure 50. Oxidation of 3.33 m DMAE/3.33 m PZ trial 2. 70 ℃, 98 kPa O2, 2 kPa CO2, 100 ml/min gas flow, 1400 rpm , 0.4 mM of Fe^{3+}, 0.2 mM Mn^{2+}, 0.1 mM Ni^{2+}, and 0.05 mM Cr^{3+}.

ICP experiments were conducted to verify whether metal concentration remains constant in all samples, and that was the case as shown in figure 43. Concentration of Ni^{2+} and Cr^{3+} remained relatively constant but concentration of Fe^{3+} and Mn^{2+} followed the trend of parent amine concentration. The ICP results suggest that the trend seen in figure 42 is likely due to water balance instead of parent amine degradation. Therefore, DMAE is resistant to oxidation.

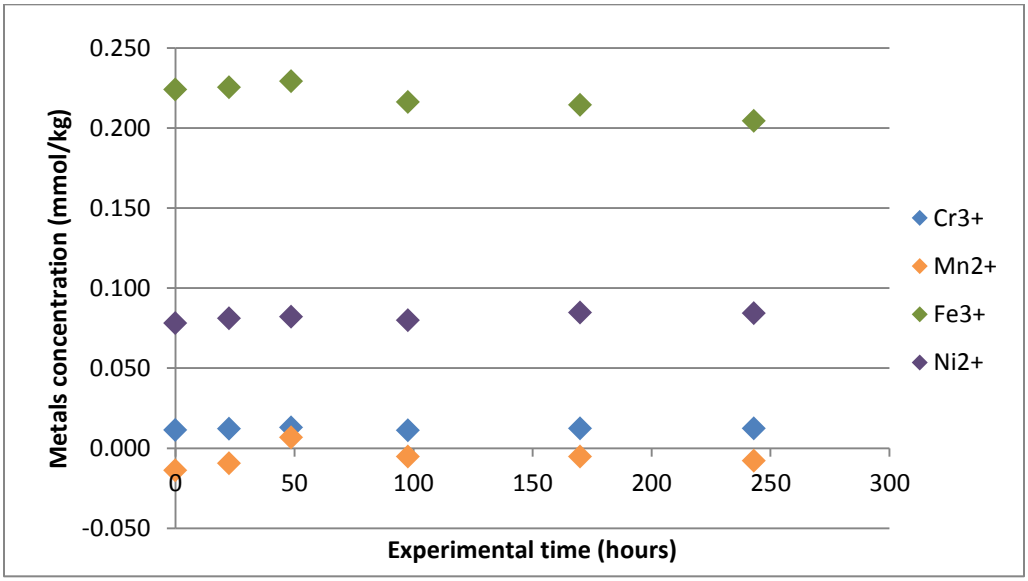

Figure 51. Metals concentration in 3.33 m DMAE/3.33 m PZ trial 2. 70 ℃, 98 kPa O2, 2 kPa CO2, 100 ml/min gas flow, 1400 rpm , 0.4 mM of Fe^{3+}, 0.2 mM Mn^{2+}, 0.1 mM Ni^{2+}, and 0.05 mM Cr^{3+}.

Concentration of oxalate in the second trial of DMAE is almost negligible except in the last sample. Formate concentration increased steadily but the value is much smaller compared to that seen in amines susceptible to oxidation. Nitrite was not detected using anion chromatography. Total formate and oxalate results confirm that DMAE produced negligible amount of degradation products and was therefore resistant to oxidation. No nitrite peak existed in anion chromatography.

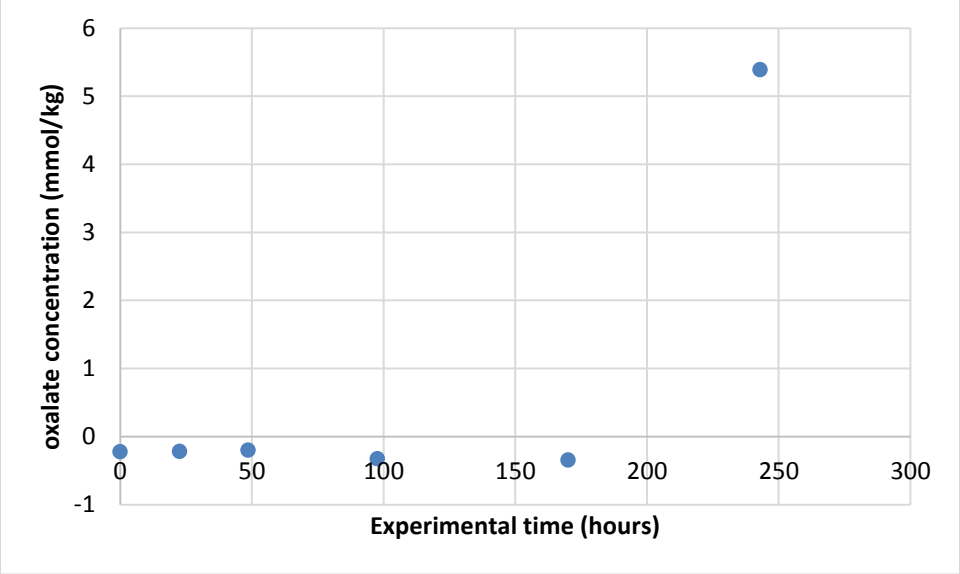

Figure 52. Oxidation product (oxalate) of 3.33 m DMAE/3.33 m PZ trial 2. 70 ℃, 98 kPa O2, 2 kPa CO2, 100 ml/min gas flow, 1400 rpm , 0.4 mM of Fe^{3+}, 0.2 mM Mn^{2+}, 0.1 mM Ni^{2+}, and 0.05 mM Cr^{3+}.

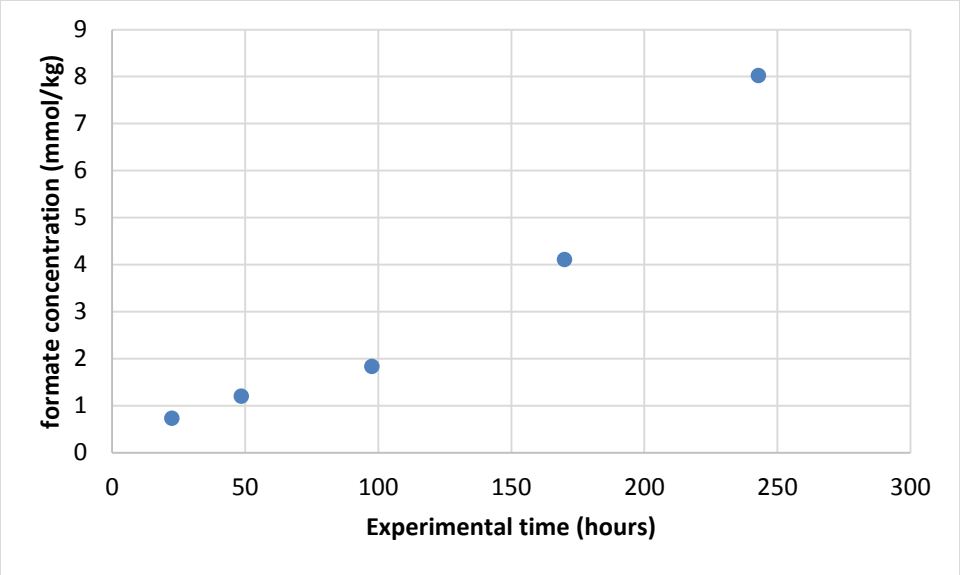

Figure 53. Oxidation product (formate) of 3.33 m DMAE/3.33 m PZ trial 2. 70 ℃, 98 kPa O2, 2 kPa CO2, 100 ml/min gas flow, 1400 rpm, 0.4 mM of Fe^{3+}, 0.2 mM Mn^{2+}, 0.1 mM Ni^{2+}, and 0.05 mM Cr^{3+}.

3.33 m 3-Dimethylamino-1-propanol /3.33 m piperazine (DMAP/PZ)

The amine of interest is DMAP, but DMAP needed to be blended with PZ because CO_2 absorption rate of DMAP alone was slow. PZ acted as a rate promoter of CO_2 absorption. Negligible degradation was observed in DMAP. Fluctuation in amine concentration over time is likely due to water balance adjustments. These results agreed with Voice's work on tertiary amine's oxidative stability.

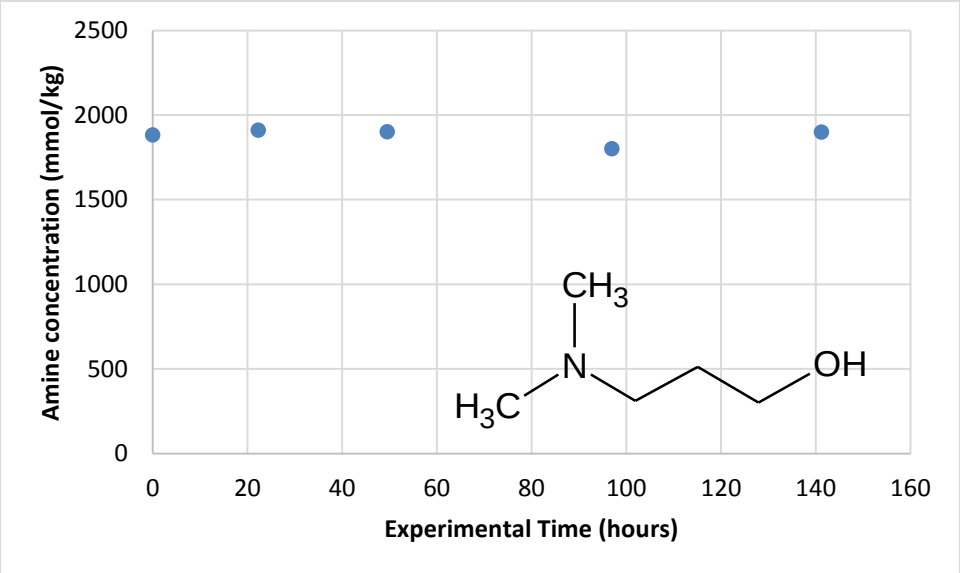

Figure 54. Oxidation of 3.33 m DMAP/3.33 m PZ. 70 ℃, 98 kPa O2, 2 kPa CO2, 100 ml/min gas flow, 1400 rpm, 0.4 mM of Fe^{3+}, 0.2 mM Mn^{2+}, 0.1 mM Ni^{2+}, and 0.05 mM Cr^{3+}.

Oxalate is not quantifiable and and formate concentrations in DMAP samples are negligible. No nitrite peak existed in anion chromatography. These data suggests that DMAP resists oxidation and agrees with conclusions drawn from cation chromatography results.

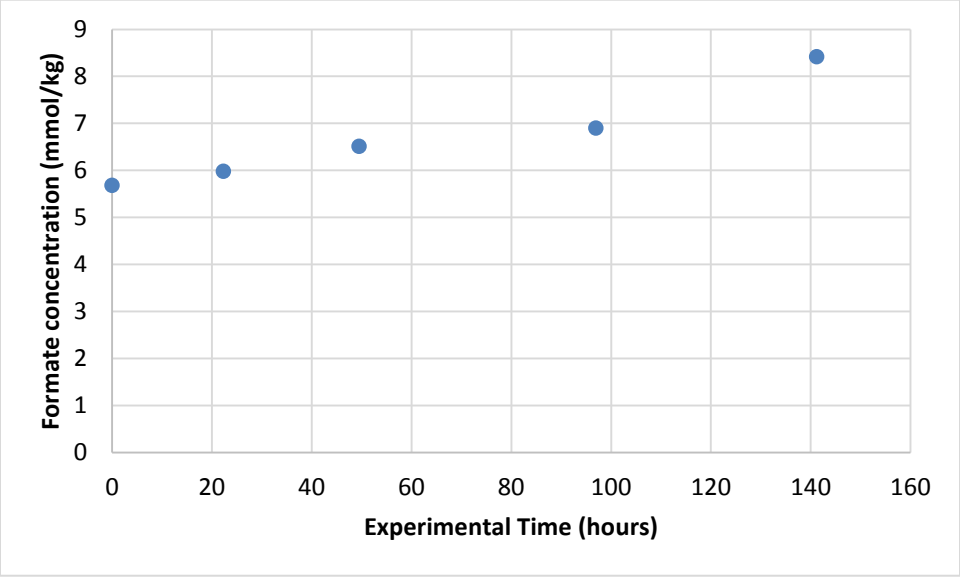

Figure 55. Oxidation product (formate) of 3.33 m DMAP/3.33 m PZ. 70 ℃, 98 kPa O2, 2 kPa CO2, 100 ml/min gas flow, 1400 rpm, 0.4 mM of Fe^{3+}, 0.2 mM Mn^{2+}, 0.1 mM Ni^{2+}, and 0.05 mM Cr^{3+}.

CONCLUSION

- This thesis focuses on the oxidative degradation of amine solvents used in coal-fired power plant flue gas CO_2 capture. The relationship between amine structures and their oxidative degradation was studied at low temperature absorber conditions in order to identify stable amines that should be more rigorously screened.
- Amongst primary amines, those with three carbons separating the two amino groups (PDA) or the amino group from the hydroxyl group (MPA) seem to be less susceptible to oxidation compared to amines with an even number of carbons separating the amino group from the neighboring electron-withdrawing group (MEA, EDA, DAB, HMDA, Jeffamine®, DGA®). Most primary amine degradations follow 1st order rate law except EDA degradation which is mass transfer limited.
- Amongst secondary amines, DEA and MAE both showed significant degradation following 2nd order rate law. MAPA showed the greatest amine loss with no parent amine left in the last sample after ~170 hours.
- Both tertiary amines, DMAE and DMAP, showed negligible degradation.
- In amines that showed significant degradation, formate, nitrite and oxalate production closely tracked parent amine degradation. In many cases such as HMDA, DEA, MAE and MAPA, oxidation product formation initially follows a linear trend and later reaches equilibrium. These oxidation products were not quantifiable in amines that resisted oxidation.
- Formate to oxalate ratio roughly approaches a constant value over time. These ratios are different depending on the amine. The same trends are observed for amine loss to formate ratio. Understanding the mechanistic significance behind these ratios is important to understanding the mechanisms of oxidation and explaining why certain structures are resistant or susceptible to oxidation.
- Degradation trends discussed in this thesis are only specific to conditions in the LGF. Amines resistant to oxidation in the LGF should be tested at high temperatures and with cycling apparatus to study their oxidation behaviors more rigorously.

Table 3. Oxidative loss for amines tested at 70 ℃, 98 kPa O_2, 2 kPa CO_2, 100 ml/min gas flow, 1400 rpm, 0.4 mM of Fe^{3+}, 0.2 mM Mn^{2+}, 0.1 mM Ni^{2+}, and 0.05 mM Cr^{3+}.

Amine	Structure	Rate constant	Amine fraction after 50 hours	Amine fraction after 100 hours
PDA	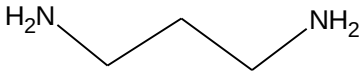	-	-	-
EDA	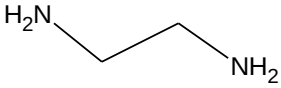	9.79 mmol/kg-hr	0.880	0.687
DAB	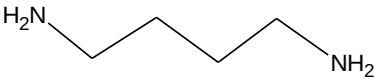	0.01 hr^{-1}	0.644	0.298
HMDA	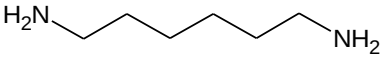	0.01 hr^{-1}	0.952	0.625
MPA	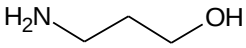	-	-	-
DGA®	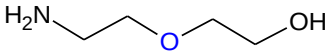	0.011 hr^{-1}	0.560	0.255
Jeffamine®	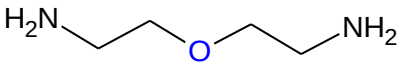	0.023 hr^{-1}	0.290	0.113
DEA	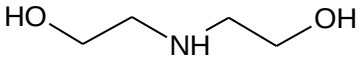	$3*10^{-6}$ $(mmol/kg-hr)^{-1}$	0.532	0.417
MAE	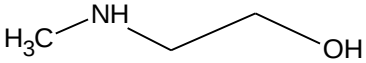	$9*10^{-7}$ $(mmol/kg-hr)^{-1}$	0.680	0.544
MEA	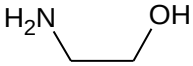	0.015 hr^{-1}	0.455	0.301

MAPA	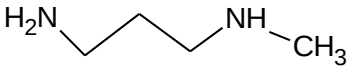	0.016 hr^{-1}	0.481	0.185
DMAE	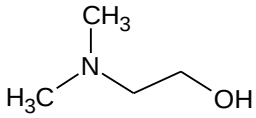	-	-	-
DMAP	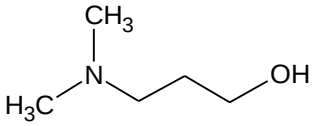	-	-	-

Table 4. Heat stable salts ratios for amines tested at 70 ℃, 98 kPa O_2, 2 kPa CO_2, 100 ml/min gas flow, 1400 rpm, 0.4 mM of Fe^{3+}, 0.2 mM Mn^{2+}, 0.1 mM Ni^{2+}, and 0.05 mM Cr^{3+}.

Amine	Structure	Formate/oxalae ratio	Amine loss/formate ratio
PDA	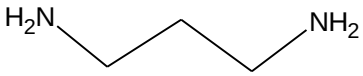	-	-
EDA	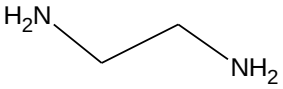	Data not available	Data not available
DAB	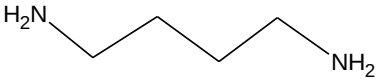	1.20	7.46
HMDA	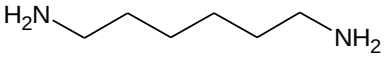	1.47	8.94
MPA	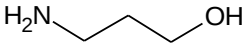	-	-
DGA®	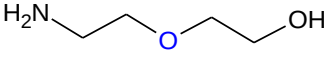	6.47	2.25
Jeffamine®	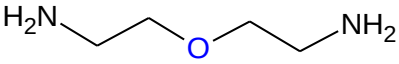	3.58	1.44

DEA	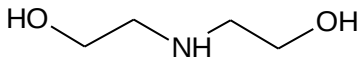	4.25	4.03
MAE	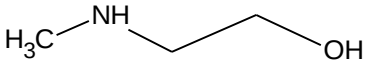	5.07	5.31
MEA	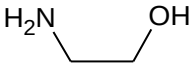	2.95	5.55
MAPA	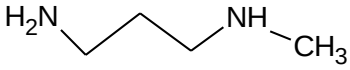	26.2	7.67
DMAE	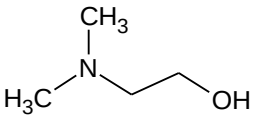	-	-
DMAP	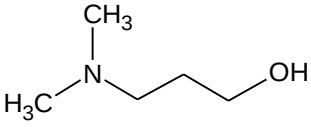	-	-

REFERENCES

Goff, G.S. (2005). *Oxidative Degradation of Aqueous Monoethanolamine in CO_2 Capture Processes: Iron and Copper Catalysis, Inhibition, and O_2 Mass Transfer* (Ph.D Dissertation). The University of Texas at Austin, Austin, Texas, USA. Retrieved from http://repositories.lib.utexas.edu

Hatchell, D.C., Carlson, M.C., Sirkar, S.D., (2015). *Thermal Degradation and Corrosion of Amines* (CHE 264 Chemical Engineering Process and Project Lab Special Project Final Report). The University of Texas at Austin, Austin, Texas, USA.

Namjoshi, O.A. (2015). *Thermal Degradation of PZ-Promoted Tertiary Amines for CO_2 Capture* (Ph.D Dissertation). The University of Texas at Austin, Austin, Texas, USA.

Sexton, A.J. (2008). *Amine Oxidation in CO_2 Capture Processes* (Ph.D Dissertation). The University of Texas at Austin, Austin, Texas, USA. Retrieved from http://repositories.lib.utexas.edu

United States Energy Information Administration (EIA). (2013, December). *Monthly Energy Review 2013*. Retrieved from http://www.eia.gov/totalenergy/data/monthly/archive/00351312.pdf

Voice, A.K. (2013a). *Amine Oxidation in Carbon Dioxide Capture by Aqueous Scrubbing* (Ph.D Dissertation). The University of Texas at Austin, Austin, Texas, USA. Retrieved from http://repositories.lib.utexas.edu

APPENDIX A. AMINES TESTED, CAS # AND MANUFACTURER

Table A.1: Amines tested, CAS # and manufacturer

Amine	Abbreviation	CAS #	Manufacturer
1,3-Diaminopropane	PDA	109-76-2	Sigma-Aldrich
Ethylenediamine	EDA	107-15-3	Sigma-Aldrich
1,4-diaminobutane	DAB	110-60-1	Sigma-Aldrich
Hexamethylenediamine	HMDA	124-09-4	Sigma-Aldrich
3-Amino-1-propanol	MPA	156-87-6	Sigma-Aldrich
Diglycolamine®	DGA®	929-06-6	Huntsman
Bis(2-aminoethyl) Ether	Jeffamine®	2752-17-2	Huntsman
Diethanolamine	DEA	111-42-2	Sigma-Aldrich
Methylaminoethanol	MAE	109-83-1	Sigma-Aldrich
Ethanolamine	MEA	141-43-5	Sigma-Aldrich
3-(Methylamino)propylamine	MAPA	6291-84-5	Sigma-Aldrich

2-Dimethylaminoethanol	DMAE	108-01-0	Sigma-Aldrich
3-Dimethylamino-1-propanol	DMAP	3179-63-3	Sigma-Aldrich

APPENDIX B. RAW DATA

Table B.1: Oxidation of 10 m MEA. 70 ℃, 98 kPa O2, 2 kPa CO2, 100 ml/min gas flow, 1400 rpm , 0.4 mM Fe, 0.2 mM Mn, 0.1 mM Ni, 0.05 mM Cr.

Time (hour)	MEA mmol/kg	Oxalate mmol/kg	Formate mmol/kg	Nitrite mmol/kg
0.0	5456	-0.02	9.52	0.37
25.4	3776	64.47	225.88	4.37
48.7	2514	131.28	469.84	11.67
70.6	1977	166.22	603.23	17.75
120.7	1407	333.30	723.24	28.79
167.6	1282	360.19	720.65	29.99
215.8	1211	298.37	842.15	29.50

Table B.2: Oxidation of 5 m PDA-5. 70 ℃, 98 kPa O2, 2 kPa CO2, 100 ml/min gas flow, 1400 rpm , 0.4 mM Fe, 0.2 mM Mn, 0.1 mM Ni, 0.05 mM Cr.

Time (hour)	PDA-5 mmol/kg	Oxalate mmol/kg	Formate mmol/kg	Nitrite mmol/kg
0.0	3244	-0.49	-0.19	0.71
23.8	3274	-0.51	-0.15	1.52
46.6	2910	-0.53	-0.06	0.73
94.5	3270	-0.47	0.06	0.66
166.8	3293	-0.46	-0.13	0.63
214.9	3264	-0.53	-0.15	0.70
262.6	3191	-0.52	0.01	0.73

Table B.3: Oxidation of 5 m MPA. 70 ℃, 98 kPa O2, 2 kPa CO2, 100 ml/min gas flow, 1400 rpm , 0.4 mM Fe, 0.2 mM Mn, 0.1 mM Ni, 0.05 mM Cr.

Time (hour)	MPA mmol/kg	Oxalate mmol/kg	Formate mmol/kg	Nitrite mmol/kg
0.0	5467	-0.45	8.90	0.67
23.3	5459	-0.51	8.78	0.68
45.8	5347	-0.56	8.69	0.73
89.9	5218	-0.53	8.39	0.72
166.5	5385	-0.39	8.89	0.62
260.0	5110	-0.37	10.13	0.79

Table B.4: Oxidation of 5 m MEA/2.5 m PDA. 70 ℃, 98 kPa O2, 2 kPa CO_2, 100 ml/min gas flow, 1400 rpm , 0.4 mM Fe, 0.2 mM Mn, 0.1 mM Ni, 0.05 mM Cr.

Time (hour)	MEA mmol/kg	Oxalate mmol/kg	Formate mmol/kg	Nitrite mmol/kg
0.0	3017	-0.36	2.21	0.60
23.8	2943	-0.32	2.96	0.70
47.2	2939	-0.22	4.53	0.76
69.8	2948	-0.03	5.37	0.74
116.7	2908	1.23	12.06	1.17
168.0	2884	1.44	11.35	1.05
237.1	2814	2.97	15.83	1.08
309.1	2791	5.60	20.57	1.10

Table B.5: Oxidation of 5 m EDA. 70 ℃, 98 kPa O2, 2 kPa CO2, 100 ml/min gas flow, 1400 rpm , 0.4 mM Fe, 0.2 mM Mn, 0.1 mM Ni, 0.05 mM Cr.

Time (hour)	EDA mmol/kg
0.0	3429
23.7	3325
46.6	3063
95.3	2409
142.3	1890
190.1	1441
238.4	1098
286.0	720
286.4	714

Table B.6: Oxidation of 5 m DAB. 70 ℃, 98 kPa O2, 2 kPa CO2, 100 ml/min gas flow, 1400 rpm , 0.4 mM Fe, 0.2 mM Mn, 0.1 mM Ni, 0.05 mM Cr.

Time (hour)	DAB mmol/kg	Oxalate mmol/kg	Formate mmol/kg	Nitrite mmol/kg
0.0	3127	2.48	8.23	0.57
22.1	2948	4.19	21.20	0.87
45.7	2117	72.38	117.59	1.31
92.7	988	224.53	277.47	8.59
165.6	417	414.78	422.70	18.05
213.1	259	360.66	403.24	19.21
263.4	183	305.50	381.89	18.48
333.9	133	500.06	481.36	21.82

Table B.7: Oxidation of 5 m HMDA. 70 ℃, 98 kPa O2, 2 kPa CO2, 100 ml/min gas flow, 1400 rpm , 0.4 mM Fe, 0.2 mM Mn, 0.1 mM Ni, 0.05 mM Cr.

Time (hour)	HMDA mmol/kg	Oxalate mmol/kg	Formate mmol/kg	Nitrite mmol/kg
0.0	1879	-0.46	1.70	0.73
24.0	1921	0.33	3.90	0.86
46.0	1839	2.41	11.33	1.34
95.6	1215	47.38	75.14	7.11
166.5	563	97.19	148.14	16.07
213.4	368	126.75	166.27	18.70

Table B.8: Oxidation of 5 m Jeffamine®. 70 ℃, 98 kPa O2, 2 kPa CO2, 100 ml/min gas flow, 1400 rpm , 0.4 mM Fe, 0.2 mM Mn, 0.1 mM Ni, 0.05 mM Cr.

Time (hour)	Jeffamine® mmol/kg	Oxalate mmol/kg	Formate mmol/kg	Nitrite mmol/kg
0.0	3062	3.72	61.91	0.61
23.4	1629	129.60	783.80	6.27
45.6	941	279.89	1460.49	15.58
93.0	357	438.12	1898.96	24.56
166.3	243	447.78	1733.44	23.80
239.7	265	578.06	2028.35	27.59
259.8	278	676.52	2394.93	32.13
330.0	309	672.13	2282.36	30.96

Table B.9: Oxidation of 5 m DGA®. 70 ℃, 98 kPa O2, 2 kPa CO2, 100 ml/min gas flow, 1400 rpm , 0.4 mM Fe, 0.2 mM Mn, 0.1 mM Ni, 0.05 mM Cr.

Time (hour)	DGA® mmol/kg	Oxalate mmol/kg	Formate mmol/kg	Nitrite mmol/kg
0.0	4406	1.10	23.94	0.53
24.7	3445	52.96	350.70	1.01
47.5	2535	120.55	722.76	4.15
99.1	1134	256.98	1456.14	13.31
119.6	945	184.15	1542.42	13.52
167.6	840	239.30	1590.49	15.41
215.3	862	285.60	1574.85	15.24

Table B.10: Oxidation of 5 m DEA. 70 ℃, 98 kPa O2, 2 kPa CO2, 100 ml/min gas flow, 1400 rpm , 0.4 mM Fe, 0.2 mM Mn, 0.1 mM Ni, 0.05 mM Cr.

Time (hour)	DEA mmol/kg	Oxalate mmol/kg	Formate mmol/kg	Nitrite mmol/kg

0.0	4688	-0.52	2.01	0.65
25.6	3197	3.07	47.50	2.60
48.5	2510	76.58	257.79	4.87
73.9	2198	33.97	256.21	6.67
96.7	1969	142.33	507.62	7.67
169.5	1703	161.78	734.92	10.27
220.0	1648	208.76	890.69	11.80
263.4	1432	213.80	990.16	12.34

Table B.11: Oxidation of 5 m MAE. 70 ℃, 98 kPa O2, 2 kPa CO2, 100 ml/min gas flow, 1400 rpm , 0.4 mM Fe, 0.2 mM Mn, 0.1 mM Ni, 0.05 mM Cr.

Time (hour)	MAE mmol/kg	Oxalate mmol/kg	Formate mmol/kg	Nitrite mmol/kg
0.0	6852	-0.47	2.30	0.64
23.9	5214	24.66	123.10	3.15
48.4	4693	43.53	250.15	4.09
96.4	3756	85.19	404.78	4.75
166.8	3150	131.75	649.10	5.03
216.4	2793	156.27	758.79	4.92
263.0	2520	173.10	887.35	5.07

Table B.12: Oxidation of 5 m MAPA. 70 ℃, 98 kPa O2, 2 kPa CO2, 100 ml/min gas flow, 1400 rpm , 0.4 mM Fe, 0.2 mM Mn, 0.1 mM Ni, 0.05 mM Cr.

Time (hour)	MAPA mmol/kg	Oxalate mmol/kg	Formate mmol/kg	Nitrite mmol/kg
0.0	3005	0.05	-0.13	0.69
25.9	2020	1.97	56.25	4.10
46.8	1505	5.46	136.95	6.55
70.8	1066	9.75	247.03	8.66
96.4	588	12.54	322.37	10.90
168.9	-23	101.96	1141.69	17.31

Table B.13: Oxidation of 3.33 m DMAE/3.33 m PZ trial 1. 70 ℃, 98 kPa O2, 2 kPa CO2, 100 ml/min gas flow, 1400 rpm , 0.4 mM Fe, 0.2 mM Mn, 0.1 mM Ni, 0.05 mM Cr.

Time (hour)	DMAE mmol/kg
0.0	390
24.5	292
47.4	249

120.8	248
166.7	246
192.3	220
217.5	232

Table B.14: Oxidation of 3.33 m DMAE/3.33 m PZ trial 2. 70 ℃, 98 kPa O2, 2 kPa CO2, 100 ml/min gas flow, 1400 rpm , 0.4 mM Fe, 0.2 mM Mn, 0.1 mM Ni, 0.05 mM Cr.

Time (hour)	DMAE mmol/kg	Oxalate mmol/kg	Formate mmol/kg
0.0	2140	-0.23	-0.04
22.5	2084	-0.22	0.73
48.6	1997	-0.20	1.20
97.7	2030	-0.33	1.83
170.1	1887	-0.34	4.10
243.0	1795	5.39	8.02

Table B.15: Oxidation of 3.33 m DMAP/3.33 m PZ. 70 ℃, 98 kPa O2, 2 kPa CO2, 100 ml/min gas flow, 1400 rpm , 0.4 mM Fe, 0.2 mM Mn, 0.1 mM Ni, 0.05 mM Cr.

Time (hour)	DMAP mmol/kg	Oxalate mmol/kg	Formate mmol/kg
0.0	1882	-0.17	5.68
22.4	1911	-0.17	5.98
49.5	1901	-0.10	6.51
97.0	1801	0.30	6.90
141.3	1899	-0.12	8.42